Fall 2019

Geophysical imaging beneath Lake Chesterfield, Missouri

James Daniell Hayes

GEOPHYSICAL IMAGING BENEATH LAKE CHESTERFIELD, MISSOURI

by

JAMES DANIELL HAYES

A THESIS

Presented to the Faculty of the Graduate School of the

MISSOURI UNIVERSITY OF SCIENCE AND TECHNOLOGY

In Partial Fulfillment of the Requirements for the Degree

MASTER OF SCIENCE IN GEOLOGICAL ENGINEERING

2019

Approved by:

Dr. Neil Anderson, Advisor
Dr. Robert Tucker
Dr. Evgeniy Torgashov

ABSTRACT

Lake Chesterfield in Wildwood, Missouri, has been leaking since construction of the earth-fill dam was completed in 1986, despite numerous mitigation efforts. The mitigation efforts, including the injection of grouting and the emplacement of clay liners, has not solve the leakage problem.

In the current study, geophysical (subsurface imaging) data was acquired across the drained and dry lake bed and along the base of the earth-fill dam to 1) map variable depth to top of bedrock, 2) determine the variable quality of the bedrock to depths on the order of 80 ft., 3) identify any significant karst features beneath the lake, and 4) identify any probable seepage pathways. These imaging data would assist geotechnical engineering firms in determining the most appropriate mitigation plan.

During the geophysical survey, electrical resistivity tomography (ERT), multi-channel analysis of surface waves (MASW), and spontaneous potential (SP) data were acquired across the drained and dry lake bed.

Interpretation of the geophysical data indicates the average depth to bedrock beneath the lake bottom is generally between 5 and 10 ft. The quality of the shallow and predominantly limestone bedrock (depths less than 30 ft.) beneath the lake bed is highly variable. In some places it is highly weathered; elsewhere it is relatively intact.

The acquired geophysical data indicate the earth-fill dam was constructed, in places, on highly weathered limestone. Three prominent low resistivity zones were mapped along the base of the earth-fill dam. It is likely that these three zones represent drainage pathways beneath the dam.

ACKNOWLEDGEMENTS

I would like to express my deep appreciation and respect to my advisor, Dr. Neil Anderson, for his patience and assistance during the process of this research. I would also like to extent my appreciation towards Dr. Evgeniy Torgashov and Dr. Robert Tucker for their assistance and guidance on this project. Finally, thanks also go to Jiawei Li, Marshal Foster, Abdullah Hadi, Katelyn and Marc Radloff, and my lovely wife Josie Clark for all the assistance they have provided me over this period.

TABLE OF CONTENTS

Page

ABSTRACT iii

ACKNOWLEDGEMENTS iv

LIST OF ILLUSTRATIONS viii

LIST OF TABLES x

SECTION

1. INTRODUCTION 1

1.1. CONSTRUCTION OF LAKE CHESTERFIELD AND THE NORTH DAM 2

1.2. PREVIOUS CONCERNS 4

1.3. CURRENT CONCERNS AND INVESTIGATION 8

2. GEOLOGICAL SETTING OF STUDY AREA 9

2.1. STRATIGRAPHY OF WILDWOOD STUDY AREA 9

2.2. OVERVIEW OF KARST TERRAIN AND SINKHOLE FORMATION 10

3. GEOPHYSICAL STUDY 13

3.1. 2-D ELECTRICAL RESISTIVITY TOMOGRAPHY (ERT) 13

3.1.1. Basic Principals and Philosophy of 2-D ERT. 13

3.1.2. Acquisition and Survey. 16

3.1.3. ERT Data Interpretation. 16

3.2. MULTI-CHANNEL ANALYSIS OF SURFACE WAVES (MASW).....23

3.2.1. Basic Principles and Philosophy of MASW.....23

3.2.2. Acquisition and Survey. 28

3.2.3. MASW Data Interpretation. 29

3.3. SPONTANEOUS POTENTIAL (SP) 31

3.3.1. Basic Principles of SP. 31

3.3.2. Acquisition and Survey. 32

3.3.3. SP Data Interpretation. 32

4. CONCLUSIONS 35

4.1. DEPTH TO TOP OF BEDROCK 35

4.2. QUALITY OF BEDROCK 35

4.3. KARST FEATURES.....36

4.4. SEEPAGE PATHWAYS 36

4.4.1. Seepage Beneath the Dam 37

4.4.2. Seepage Vertically. 37

4.4.3. Seepage Laterally. 37

5. RECOMMENDATIONS 38

APPENDICES

A. ERT PROFILES, NNE-SSW 1-12 AND W-E 13-15 WITH INTERPRETATIONS 39

B. MASW PROFILES 2, 3 8, 9, AND 11 WITH INTERPRETATIONS 55

BIBLIOGRAPHY 61

VITA 63

LIST OF ILLUSTRATIONS

Page

Figure 1.1. Google Earth image of Lake Chesterfield and North Dam 3

Figure 1.2. North Dam cross-section 3

Figure 1.3. Locations of previous sinkholes, exploratory borings and grout injection points 6

Figure 1.4. Photo A and B of 2004 sinkhole and remediation 7

Figure 2.1. Approximate location of Lake Chesterfield (yellow) within Wildwood (red) in St. Louis County. 9

Figure 2.2. Boring logs 024175 and 023103 near the approximate location of Lake Chesterfield. 10

Figure 2.3. Process of sinkhole formation 11

Figure 2.4. Location of all known sinkholes in Missouri 12

Figure 3.1. Resistivity ranges of commonly found soils, rocks and minerals 14

Figure 3.2. Basic ERT array with four electrodes to measure the subsurface resistivity. 14

Figure 3.3. Dipole-dipole electrode geometry 15

Figure 3.4. ERT traverse locations from T1-T17 (red lines), MASW (1-11), and SP base electrode locations in Lake Chesterfield 17

Figure 3.5. Example of an ERT profile, traverse 3 18

Figure 3.6. Variations in the elevation of top of rock as per the interpretations of the acquired ERT data 19

Figure 3.7. NNE-SSW orientated ERT traverses 1-12. 21

Figure 3.8. Northern W-E orientated ERT traverses 13-15 22

Figure 3.9. Overview of MASW data processing 25

Figure 3.10. Particle motion of different waves 26

Figure 3.11. Typical geometry used for MASW data acquisition 28

Figure 3.12. 1-D 10-layer model of shear-wave velocity profile of MASW profile 3 30

Figure 3.13. Schematic set-up and collection of SP data. 33

Figure 3.14. (a) Induced negative electrokinetic potential associated with the flow of water in the ground. (b) SP map in plane view 33

Figure 3.15. Contoured SP data overlaid on Lake Chesterfield 34

LIST OF TABLES

Page

Table 3.1. NEHRP Site Classification Guidelines for soil and rock. 24

1. INTRODUCTION

Lake Chesterfield, located in Wildwood, Saint Louis, Missouri, is a small homeowner's association lake owned operated by the Lake Chesterfield Home Owners Association (LCHOA). Construction of the lake, including the dam, was completed in 1987.

Lake Chesterfield has been leaking, more-or-less continuously, since it was constructed. Numerous mitigation efforts throughout 1988, 1994, 1995, 2004, and 2005 to mitigate the leaks, including the grouting the interpreted leakage zones and the emplacement of clay liners, have failed to stem the leakage for long. In 2017, LCHOA contacted Missouri S&T with the aim of finding a permanent solution to the leakage issues.

In the late spring of 2018, Lake Chesterfield was drained in preparation for the Missouri S&T geophysical survey. Geophysical investigations are often cost-effective methods for investigating the shallow subsurface (i.e. depths <100 ft.). The geophysical tools selected for the Lake Chesterfield survey included 2-D electrical resistivity tomography (ERT), multi-channel analysis of surface waves (MASW), and spontaneous potential (SP). These methods were used with the purpose to 1) map variable depth to top of bedrock, 2) determine the variable quality of the shallow bedrock, 3) identify any significant karst features beneath the lake, and 4) identify any probable seepage pathways.

1.1. CONSTRUCTION OF LAKE CHESTERFIELD AND THE NORTH DAM

Lake Chesterfield was constructed to provide storm water retention and recreation for the residents in the area. Situated at the headwaters of Caulk Creek, which drains north into the Missouri River, the lake spans 20 acres at maximum fill, is approximately 2200 ft. long and 450 ft. wide at the widest point. The lake is bordered by two dams – a North Dam and a South Dam (Figure 1.1). The North Dam is the area of primary concern and discussion of the South Dam is not relevant to this study.

The North Dam is 32 ft. in height and 700 ft. long. A road, Pierside Lane, runs atop the crest of the dam (Figure 1.1). The base of the dam is at an elevation of approximately 640 ft. The dam was constructed with a clay core with the remaining earth fill consisting of silt, sand, gravel and clay (Eckelkamp, 1986).

Prior to construction, a 5 ft. deep cutoff trench (Figure 1.2) was extended into the native soil. The dam was constructed on what was identified, at the time and in auger borings, as bedrock. Based on the interpretation of the geophysics data acquired during the current 2018 investigation, it is concluded that the upper 30 ft. of rock beneath the dam, in places, is highly weathered limestone.

The lake bottom was covered with a clay blanket on the lake bed with the expectation the dam would not leak, and the lake would retain water.

Figure 1.1. Google Earth image of Lake Chesterfield and North Dam.

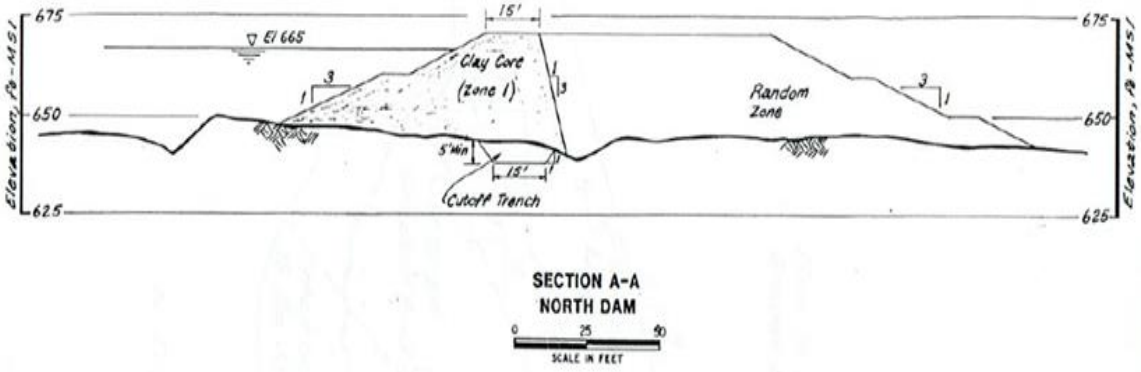

Figure 1.2. North Dam cross-section (Eckelkamp, 1986). Elevations and distances are in feet.

1.2. PREVIOUS CONCERNS

The following information was compiled from previous reports prepared by; Eckelkamp, (1986), Taylor, (2005), and Wieners, and Kremer (2005).

The Eckelkamp (1986) geotechnical report recognized that the construction location for the lake and dam was in a karst area.

Three sinkholes were discovered in 1986 on the northern section of the lake when the area was initially graded (Figure 1.3). Two of the sinkholes were on the western side of the lake near the tennis courts. One of the two sinkholes on the western edge was excavated down to a depth of 20 ft. where a karst trench trending NNE/SSW was discovered. This sinkhole was treated by placing serval feet of 2-3in rock in the passageway, capping with concrete and backfilling. The second sinkhole on the western edge was excavated down to a depth of 35 ft. As no cavity was present the excavated sinkhole was backfilled. The third sinkhole was discovered approximately 1000 ft. south of the North Dam on the eastern side of the lake near a knoll that extends from the eastern shore. This sinkhole was sealed using graded rock filler, whereby large rocks are placed in the throat of the sinkhole and progressively smaller rocks are placed on top before backfilling with native soil.

A zone of leakage was identified on the lake in 1995 (Figure 1.3). This zone of leakage was believed to be parallel to the eastern shore. The geophysical company Strata Services, Inc. was hired to grout the seepage pathway. Nine grout holes were drilled and 4144 cubic feet of neat cement/pozzolan slurry and 1620 cubic feet of sand-cement/pozzolan slurry were injected.

In 1996, four additional grout holes were drilled to plug another identified seepage pathway in immediate proximity to the 1995 grout holes (Taylor, 2005). The Taylor report does not indicate the specific location of the four grout holes, so the locations cannot be superposed on the map of Figure 1.3. At that time, water leakage from the lake was estimated to be in the range of 100-300 gallon per minute. 1036 cubic feet of neat cement/pozzolan slurry and 324 cubic feet of sand-cement/pozzolan slurry were injected into the four grout holes. Once grouting was completed, leakage rates decreased substantially (Taylor, 1996).

In 2000, a subsidence feature with associated leakage developed in the NE section of the dam (Figure 1.3). A total of five grout holes were drilled. Grout was injected at an angle of 12 degrees oriented towards the lake to penetrate underneath the subsidence feature. 796 cubic feet of neat cement/pozzolan slurry and 486 cubic feet of sand-cement/pozzolan slurry were injected. Strata Services, Inc. concluded that this grout curtain should seal any leakage associated with the subsidence. Leakage was temporarily reduced.

In June 2004, a sinkhole formed at the north end of the lake (Figure 1.4). Leakage through this feature rapidly and fully drained the lake. A dye test found that the water that drained into the sinkhole emerged 3.5 miles north of the lake at Lewis Spring. This suggests to the author that the waters that drained into the sinkhole flowed to the north beneath the dam along the original Caulks Creek pathway. This should not be surprising as bedrock beneath Caulks Creek would have been extensively weathered, in places, and would be an ideal conduit for mostly horizontally flowing water.

Shannon and Wilson, Inc. drilled 5 core holes, SW1 - SW5 (Figure 1.3) on the earth filled dam to ensure the structural integrity on the dam hadn't been compromised. The core holes indicated that the subsurface (to a depth of 48 feet in one corehole) was comprised of reddish-brown fat clay and silt with chert fragments. The underlying limestone was moderately to highly weathered limestone inbedded with shale and chert. Shannon and Wilson, Inc. concluded that the structural integrity of the North Dam had not been compromised.

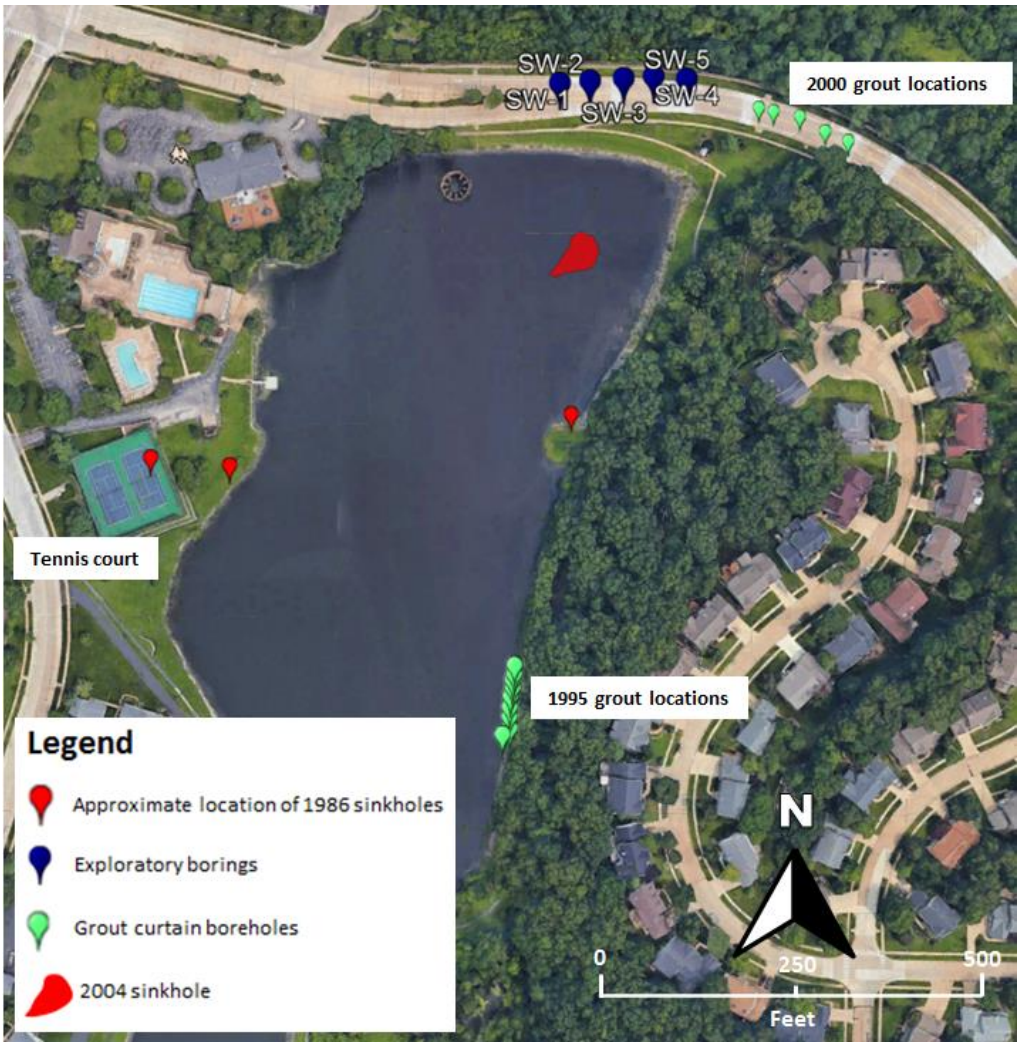

Figure 1.3. Locations of previous sinkholes, exploratory borings and grout injection points.

Figure 1.4. Photo A and B of 2004 sinkhole and remediation. A: Looking south along Lake Chesterfield, showing scale of the sinkhole and remediation. B: Sinkhole being filled with grout, in this photo you can clearly see the highly weathered limestone (Wieners, 2005).

1.3. CURRENT CONCERNS AND INVESTIGATION

Despite the previously mentioned mitigation efforts in 2017 the LCHOA noted that the leaking in the lake had increased and that the lake level frequently fell multiple inches per day. The LCHOA wanted to find a permanent solution to the ongoing leaking issues the lake has faced since construction. LCHOA asked Missouri S&T to assist in determining the source of the ongoing problems through a geological survey of the site.

In the summer of 2018 Missouri S&T acquired ERT, MASW, and SP data on the drained and dry lake bed (see Figure 3.4). Expectations were that the interpretation of the subsurface imaging data would enable help investigators to map the depth to top of bedrock, determine the variable condition of the bedrock based on variations in shear-wave velocity and electrical resistivity, locate any karst features in the subsurface beneath the lake bed, and locate any potential seepage pathways.

Based on these data, it was anticipated that a geotechnical company could develop a plan to minimize the seepage problem.

2. GEOLOGICAL SETTING OF STUDY AREA

The city of Wildwood (Figure 2.1) is a suburb in St. Louis County, Missouri. The city is situated between the Missouri River to the north, Eureka City and the Meramec River to the south, and Franklin County to the west.

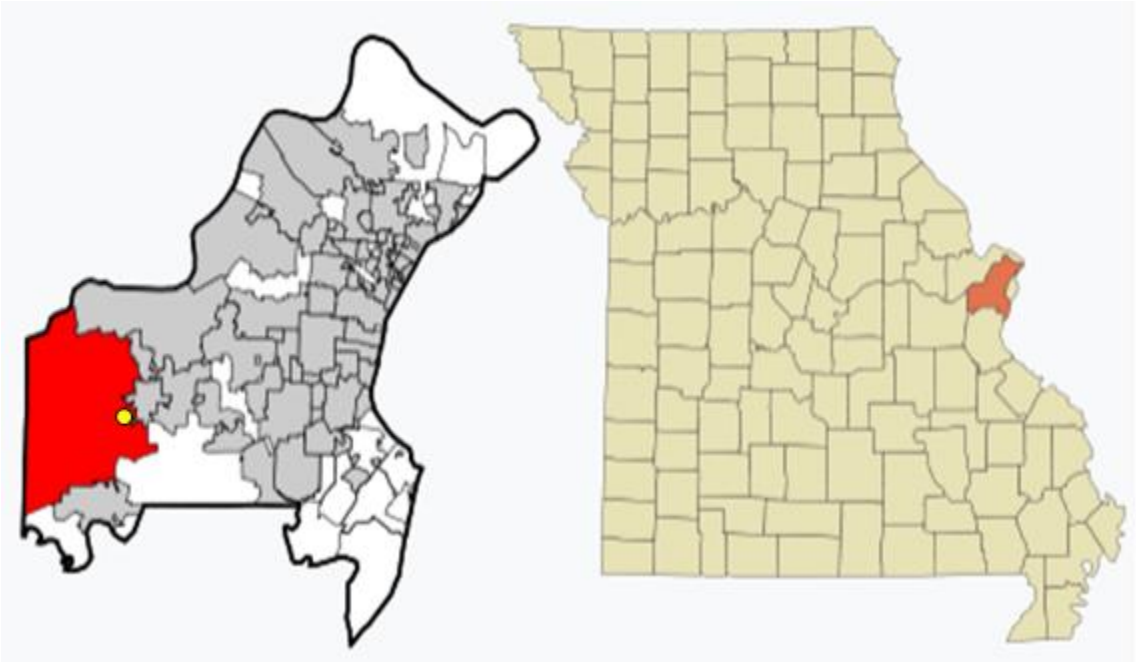

Figure 2.1. Approximate location of Lake Chesterfield (yellow) within Wildwood (red) in St. Louis County.

2.1. STRATIGRAPHY OF WILDWOOD STUDY AREA

Bedrock in the study area is the St. Louis Limestone. Bedrock (to a depth of 120 ft.) consists predominantly of limestone and dolomite imbedded with shale and chert (Figure 2.2).

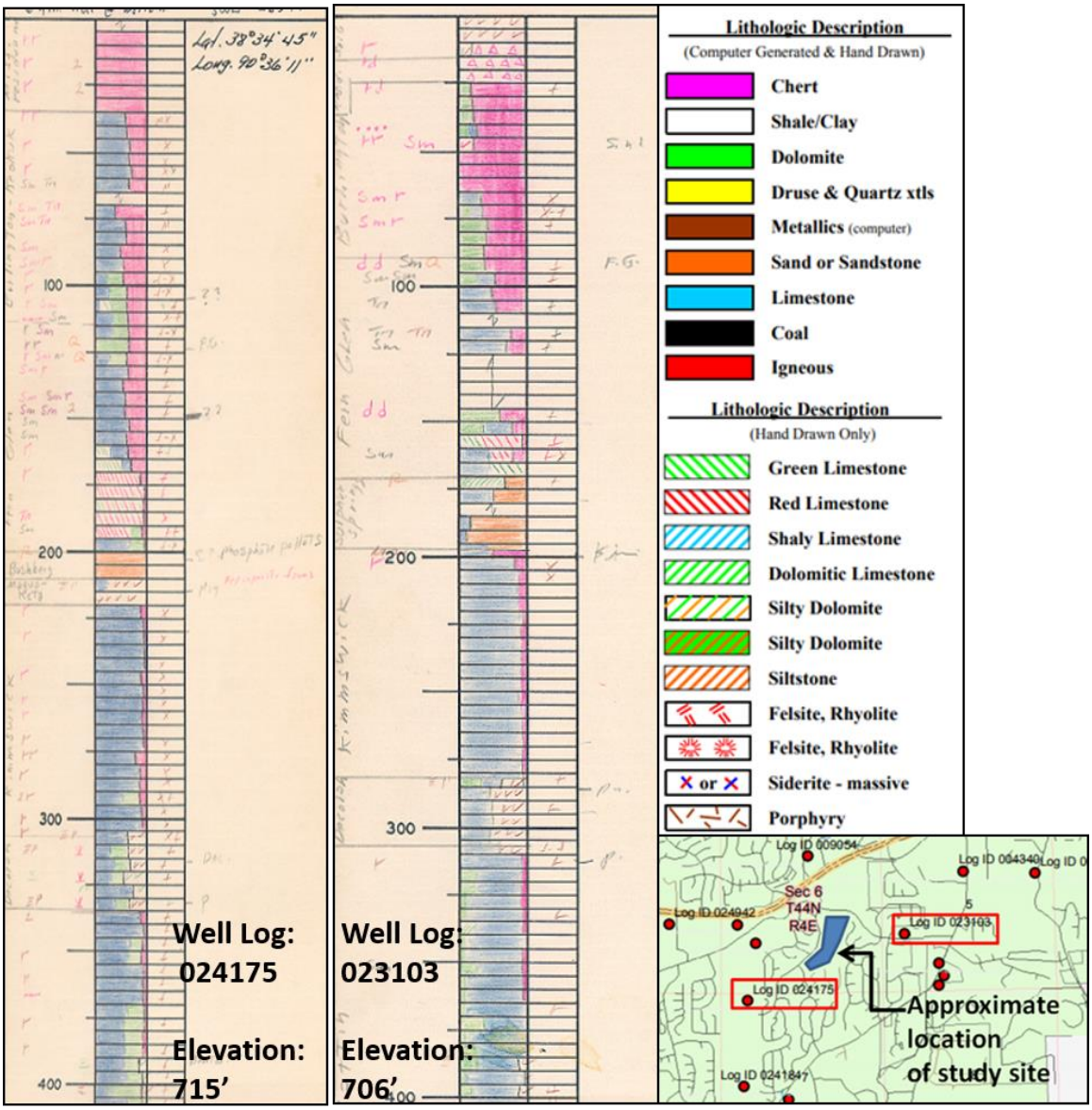

Figure 2.2. Boring logs 024175 and 023103 near the approximate location of Lake Chesterfield. (Missouri Department of Natural Resources).

2.2. OVERVIEW OF KARST TERRAIN AND SINKHOLE FORMATION

Karst is traditionally thought of as regions of soluble bedrock. Karst terrain typically manifests itself in one of three ways: (1) subsidence of the land (i.e. sinkholes);

(2) subsurface conduit systems, (i.e. fractures and solution-widened joints); or (3) discharge area (i.e. springs).

Sinkholes can pose significant hazards to people and buildings if they are not dealt with, yet they can appear seemingly out of nowhere. Sinkholes in Missouri primarily develop in the carbonate bedrock, particularly in the areas with limestone and dolomite. When rain falls, it absorbs carbon dioxide creating carbonic acid. This carbonic acidic water seeps into the subsurface and dissolves rock which is then removed with the flow of the water. As time goes on, the continuous dissolution of the rock can either create a void in which the overlaying soil layer can collapse into or whereby the removed rock is replaced by the soil, both of which will lead to surface subsidence (sinkhole formation), as seen in Figure 2.3.

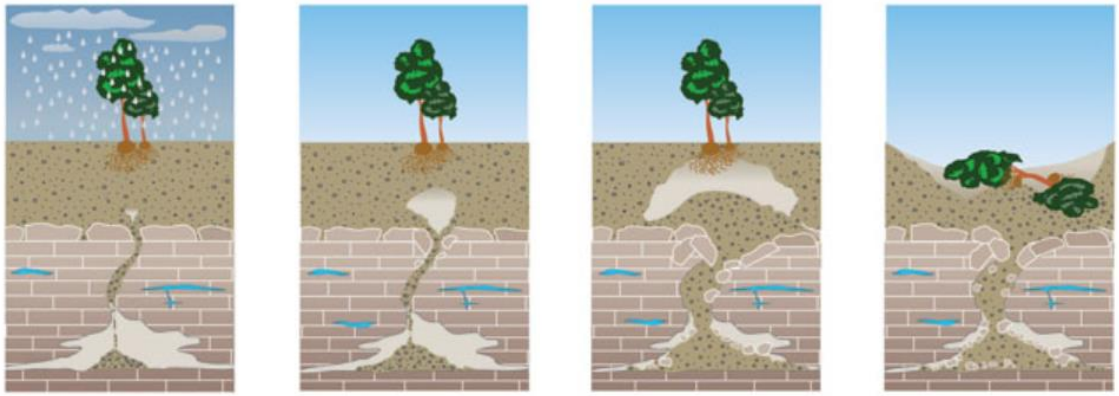

Figure 2.3. Process of sinkhole formation, from left-right, where carbonate rocks are broken-down and removed whereby the overlaying soil collapses to cause a sinkhole. (Missouri Department of Natural Resources).

It is estimated that 20% of the United States is prone to sinkhole formation, with Missouri and six other states being particularly susceptible to sinkhole formation. As of

2018, the Missouri Department of Natural Resources has verified upwards of 15,000 sinkholes in Missouri alone (Figure 2.4).

Figure 2.4. Location of all known sinkholes in Missouri, with St. Louis County in red; each yellow dot represents a sinkhole. (Missouri Department of Natural Resources).

3. GEOPHYSICAL STUDY

For this study, three geophysical tools - electrical resistivity tomography (ERT), multi-channel analysis of surface waves (MASW) and spontaneous potential (SP)– were employed. The data were gathered, processed and interpreted as described in the following sections.

3.1. 2-D ELECTRICAL RESISTIVITY TOMOGRAPHY (ERT)

2-D Electrical resistivity tomography (herein referred to simply as ERT) is a non-destructive imaging technique used to measure lateral and vertical variations the resistivity of the subsurface. The resistivity of earth material can help qualify and quantify the nature of that material. Resistivity ranges of common soils, rocks, and minerals can be seen in Figure 3.1. In the study area moist clay soils and limestone are the predominant materials present as stated in the reports and borings logs of previous reports.

3.1.1. Basic Principals and Philosophy of 2-D ERT. Employing ERT allows estimates of the true resistivity of the subsurface to be obtained. This is useful as the resistivity of the earth materials is related to the moisture content, clay content, lithology and rock quality.

In terms of basic concepts, during an ERT survey, a known current (I) is input into the subsurface through two electrodes (C1 and C2; Figure 3.2) and the potential difference (V) is measured using another two electrodes (P1 and P2; Figure 3.2). Generally, all the electrodes are placed along linear or nearly linear traverse.

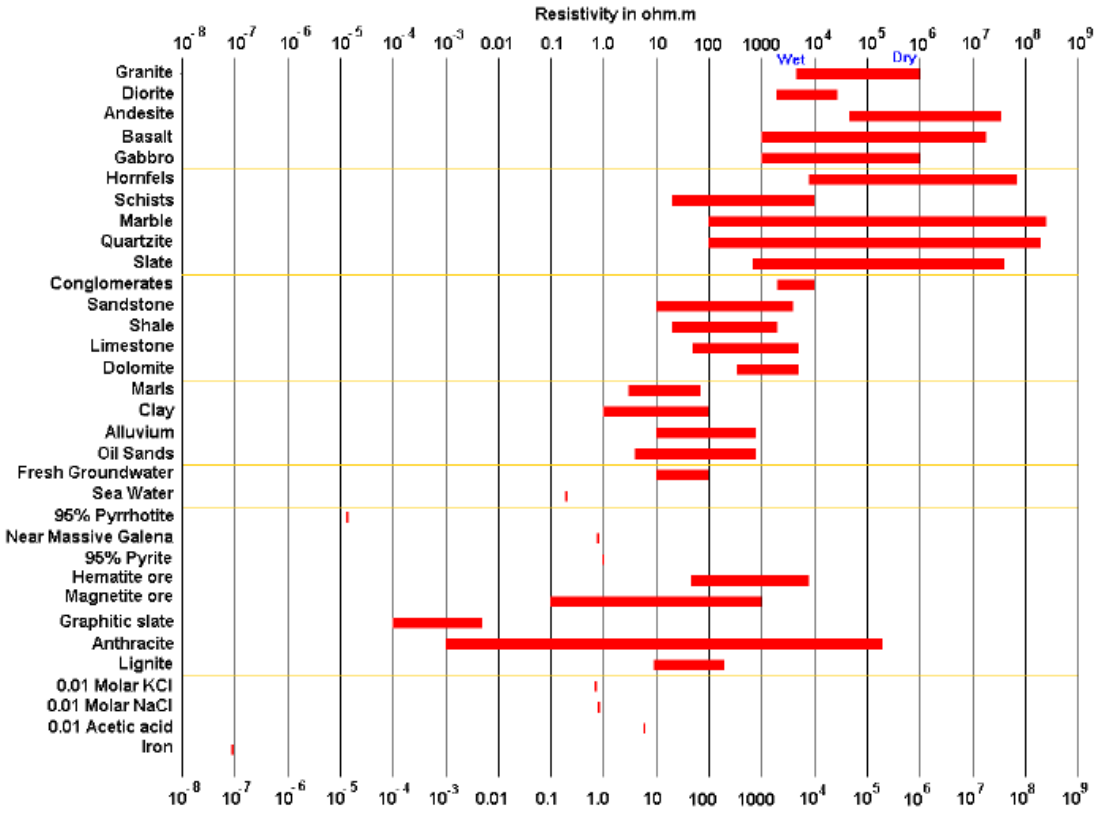

Figure 3.1. Resistivity ranges of commonly found soils, rocks and minerals (Loke, 2004).

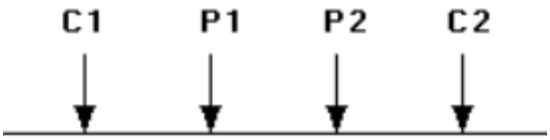

Figure 3.2. Basic ERT array with four electrodes to measure the subsurface resistivity. (Loke, 2004).

From the known current input (I) and the measured potential difference ($\Delta\emptyset$), the apparent resistivity (ρ_a) can be calculated:

$$\rho_a = k\frac{\Delta\emptyset}{I}$$

where *k* is the geometric factor of the electrode spacing:

$$k = \frac{2\pi}{\left(\frac{1}{r_{C1P1}} - \frac{1}{r_{C2P1}} - \frac{1}{r_{C1P2}} + \frac{1}{r_{C2P2}}\right)}$$

where $r_{C1P1}$is the distance from the current electrode 1 (C1) to the potential electrode 1 (P1), $r_{C2P1}$is the distance between current electrode 2 (C2) and potential electrode 1 (P1), r_{C1P2} is the distance between current electrode 1 (C1) and potential electrode 2 (P2), and r_{C2P2} is the distance between current electrode 2 (C2) and potential electrode 2 (P2) (Loke, M.H, 2004).

The electrode geometry can be installed in any configuration desired. We acquired ERT data utilizing a dipole-dipole array (Figure 3.3). As this array type is the most sensitive to the horizontal changes in resistivity (Loke, 2004).

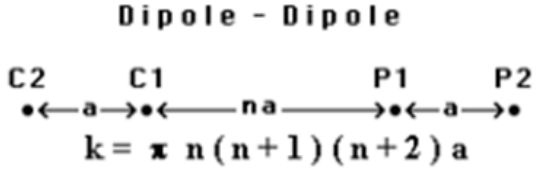

Figure 3.3. Dipole-dipole electrode geometry. Where ***k*** is the geometric factor, ***a*** dipole length, and ***n*** the dipole separation factor, commonly an integer value. (Loke, 2004).

Finally, using tomographic algorithms, the entirety of the apparent resistivity is used to generate a 2-D model of the subsurface (Figure 3.5).

3.1.2. Acquisition and Survey. The ERT survey was designed to efficiently image drained and dry northern section of Lake Chesterfield. ERT data were acquired and stored using an Advanced Geosciences, Inc. (AGI) Supersting, R8. Twelve ERT traverses (T1 – T12) were laid along the axis of the Lake Chesterfield (parallel to the old Caulks Creek bed) in an NNE-SSW direction. Five ERT traverses (T13 – T17) were laid across the width of the lake in a W-E direction (Figure 3.4). All the ERT data were acquired using uniform 5 ft. electrode spacing.

3.1.3. ERT Data Interpretation. The resistivity of earth materials in the study area is mostly a function of moisture content and clay content. Similarly, as clay content increases, resistivity decreases.

The processed ERT data, Figure 3.5, can be subdivided into four sections on the basis of resistivity: (1) clay liner and native soil (<45 Ohm-m); (2) highly weathered limestone (<75 Ohm-m); (3) weathered limestone (75-250 Ohm-m); and (4) intact limestone (>250 Ohm-m).

The clay liner and native soil is between 5 ft. and 10 ft. thick and covers the entire lake bed. As shown in Figure 3.5, the clay liner and native soil are underlain mostly by a 5 to 15 ft. thick unit of mostly weathered limestone. The top of this weathered limestone unit was classified as the top-of-rock in the test pits that were dug when the dam was originally constructed.

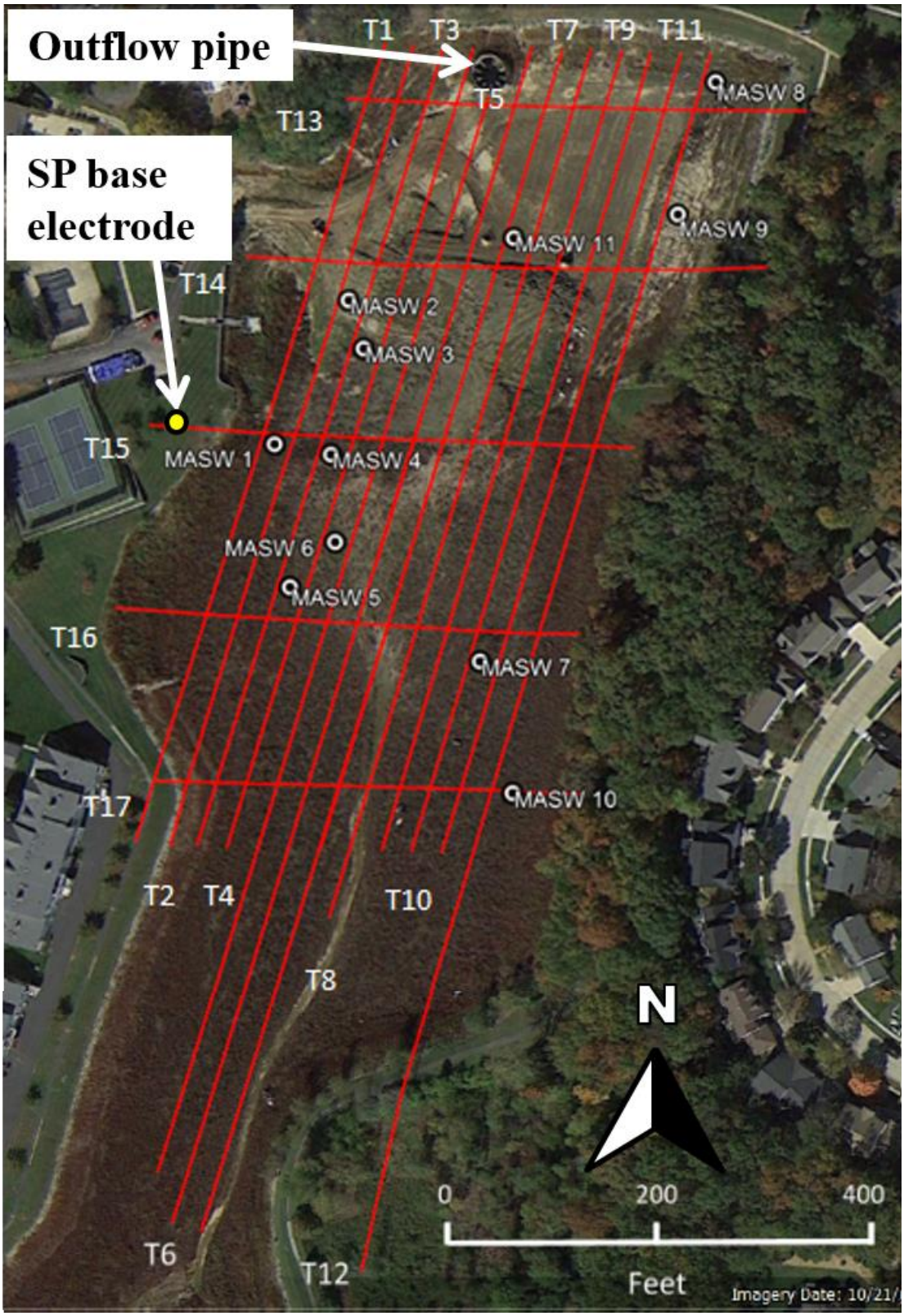

Figure 3.4. ERT traverse locations from T1-T17 (red lines), MASW (1-11), and SP base electrode locations in Lake Chesterfield (Anderson, 2018).

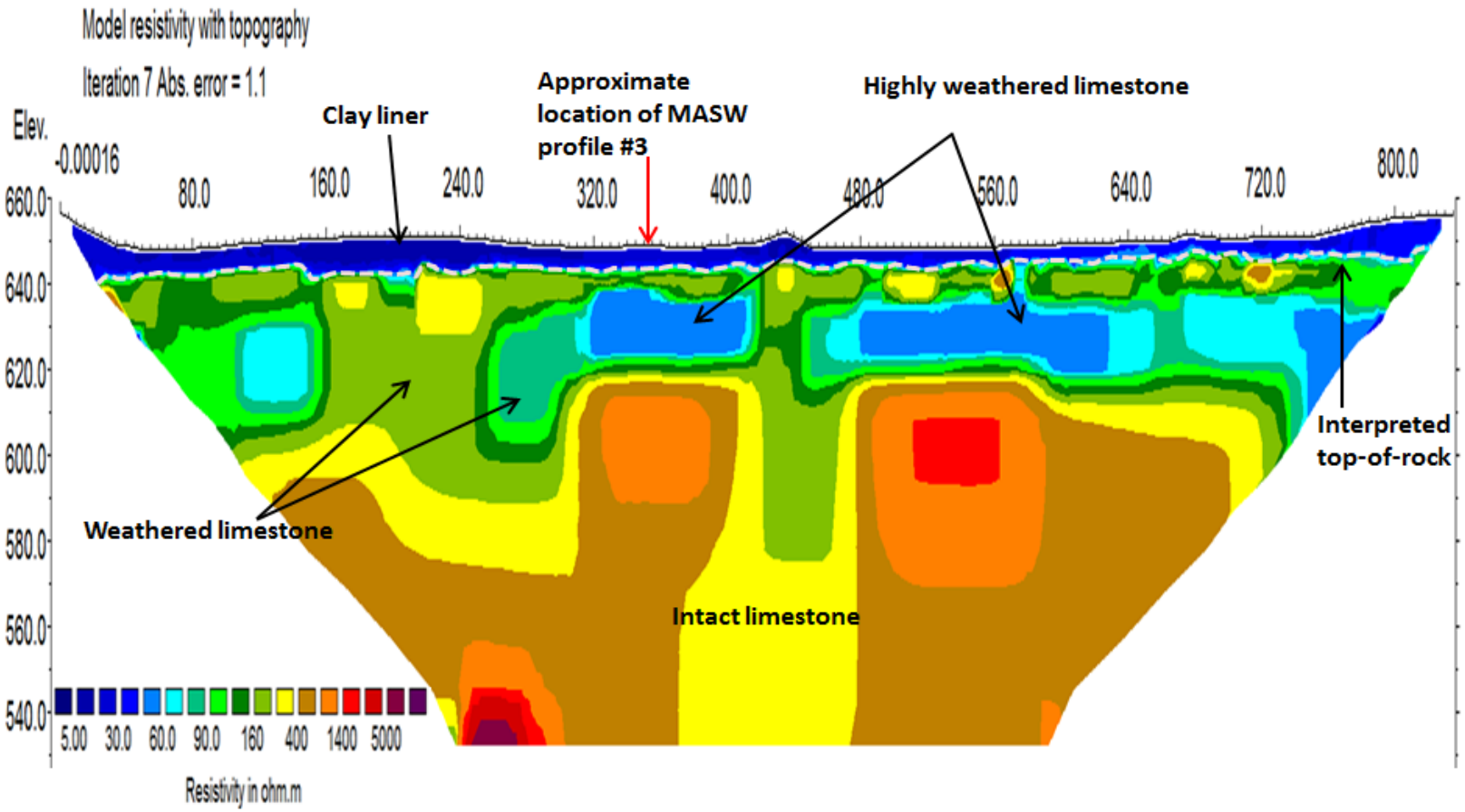

Figure 3.5. Example of an ERT profile, traverse 3 (T3 Figure 3.4) shown here. Interpreted top-of-rock shown in the dashed line corresponds with 45 Ohm-m value. Various features can be identified: intact limestone (yellow-purple) values greater than 250 Ohm-m, weathered limestone (green) values between 75-250 Ohm-m, highly weathered limestone (light blue) between 45-75 Ohm-m, and clay liner (dark blue) less than 45 Ohm-m. (Anderson, 2018).

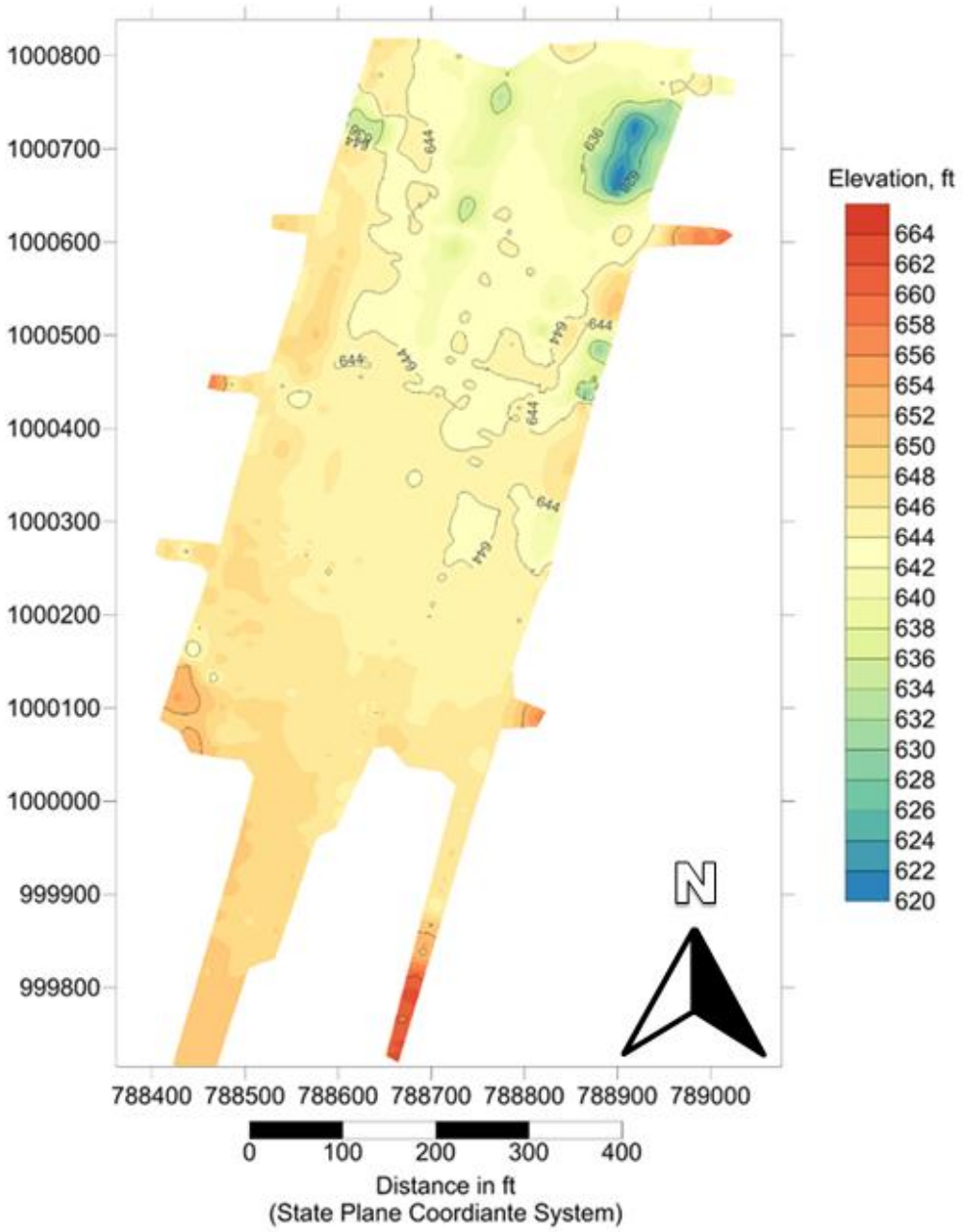

Figure 3.6. Variations in the elevation of top of rock as per the interpretations of the acquired ERT data. (Anderson, 2018).

The upper zone of mostly weathered limestone, as shown in Figure 3.5, is typically underlain by about 20 ft. of weathered to highly weathered limestone. The

acquired MASW data (Section 3.2) indicate this weathered to highly weathered unit is characterized, in places, by shear-wave velocities comparable to those of soils rather than rock. It is anticipated that this zone consists of weathered to highly weathered limestone and piped clay.

The zone of weathered to highly weathered limestone is underlain (mostly) by what is interpreted as relatively intact limestone.

As noted in the discussion section of this thesis, it is believed that the zone of weathered to highly weathered limestone extends beneath the dam and serves as a conduit for waters seeping through the lake bottom and flowing northward beneath the dam along the old Caulks Creek waterway.

A map depicting variations in depth to top-of-rock within the entire lake bed is presented as Figure 3.6. Figure 3.6 shows that the interpreted top-of-rock is relatively consistent except for the depression in the bedrock elevation in the northeast of the lake (Figure 3.6). This depression is the location of the 2004 sinkhole and subsequent remediation efforts (Figure 1.3, and 1.4).

Interpreted solution-widened joints and probable flow paths have been superposed on the ERT data (Figures 3.7 and 3.8). The solution-widened joints are vertical features and are believed to contain significant piped clay and are hence characterized by low resistivity values. The interpreted west-east trending solution-widened joints in ERT traverses 1-12 (Figure 3.7) are more or less perpendicular to Caulks Creek. It is anticipated that the solution-widened joints are clay filled and pinch out at depth and that significant volumes of water do not drain along these vertical joints.

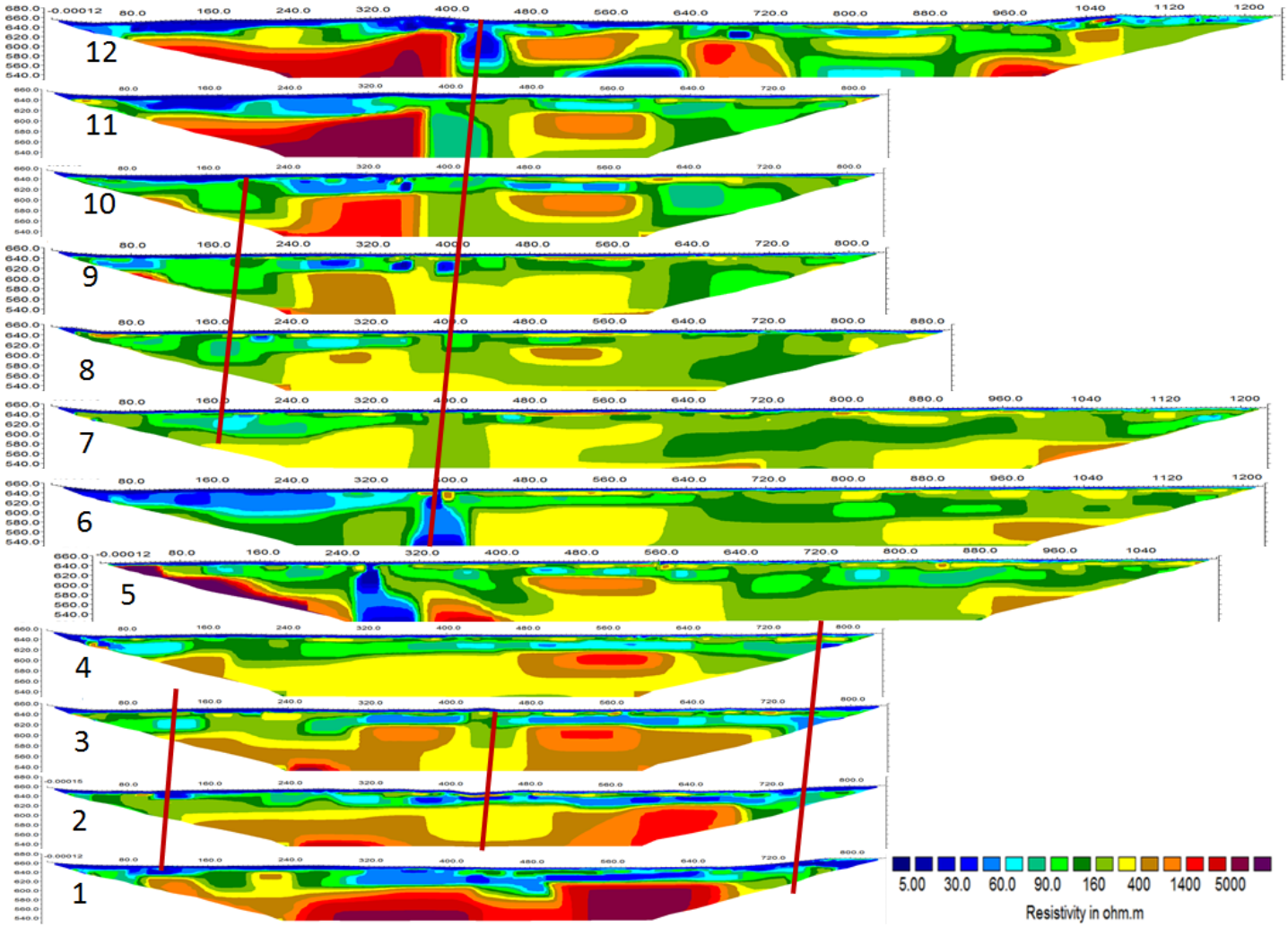

Figure 3.7. NNE-SSW orientated ERT traverses 1-12. Red lines are interpreted solution-widened joints linking the traverses. (Anderson, N.L, 2018). North end of traverses are to the left, elevations and distances are in feet.

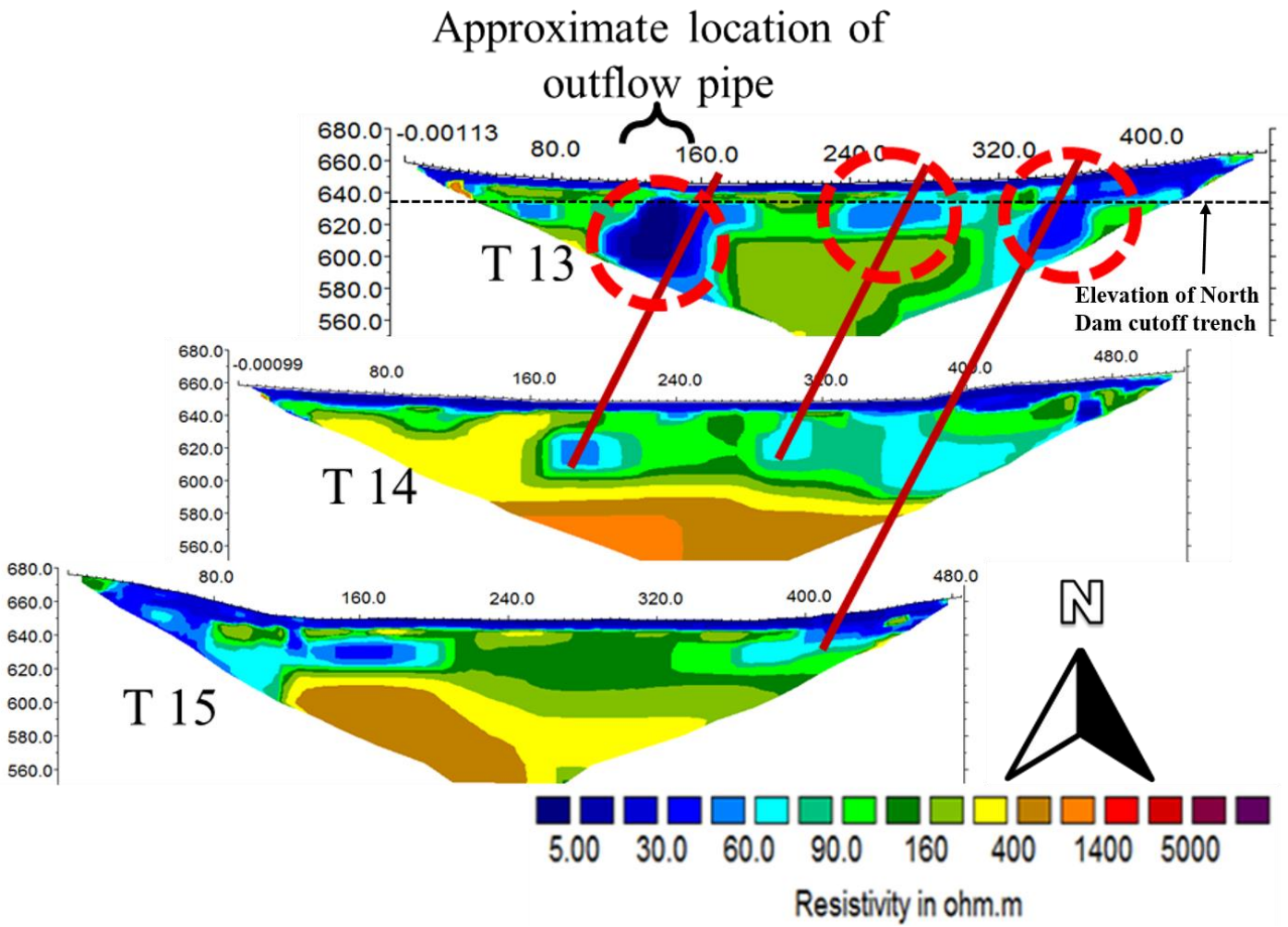

Figure 3.8. Northern W-E orientated ERT traverses 13-15. Solid red lines between traverses 13-15 are interpreted flow paths linking the traverses. Dashed red circles are possible seepage pathways beneath the dam. Dashed black line shows the base elevation of the cutoff trench (Anderson, 2018). Elevations and distances are in feet.

The horizontal low resistivity zones in ERT traverses 13-15 (Figure 3.8), are more or less perpendicular to Caulks Creek, and interpreted as horizontal flow paths. These interpreted flow paths are believed to contain significant piped clay and are hence characterized by low resistivity values. It is believed that these interpreted flow paths continue beneath the dam. If this premise is correct, then the interpreted flow paths could serve as horizontal conduits for waters flowing to the north beneath the dam along the old Caulks Creek pathway. The low resistivity values near the location of the outflow pipe could be the result of the electrical current flowing through the outflow pipe instead of the ground, this could be confirmed or not by drilling at this location.

3.2. MULTI-CHANNEL ANALYSIS OF SURFACE WAVES (MASW)

MASW is a non-destructive technique developed by the Kansas Geological Survey and is used to measure the average shear-wave velocity (Vs) of the subsurface. Using the National Earthquake Hazards Reduction Program (NEHRP) guidelines in tandem with the average Vs enables classification of the soil and rock of the subsurface by category (Table 3.1).

3.2.1. Basic Principles and Philosophy of MASW. The MASW method is designed to measure the phase velocities of Rayleigh (surface) waves. Relative to body waves, Rayleigh waves are characterized by low-velocities, low-frequencies, and high-amplitudes. Rayleigh waves are generated by striking the ground with a source, typically a 20 lb. sledge hammer or weight drop. The seismic signal generated is recorded using low-frequency vertically polarized geophones coupled to the ground. Each geophone produces a single trace signal, which is compiled within the computer software. A phase velocity

versus frequency profile (dispersion curve) is created from the information in the computer software. After the dispersion curve is identified, a 1-D vertical shear wave velocity profile may be generated for that MASW data set (Figure 3.9).

Table 3.1. NEHRP Site Classification Guidelines for soil and rock.

Site Class	General description	Detailed Description	Shear Wave velocity	
			m/sec	ft/sec
A	Hard Rock	Includes unweathered intrusive igneous rock. Soil types A and B do not contribute greatly to shaking amplification.	> 1,500	> 5,000
B	Rock	Volcanics, slightly weathered intrusive igneous, and high-grade crystalline metamorphic bedrock (upper range) to well-cemented and lithified coarse-grained sedimentary or low-grade metamorphic rock (lower range)	750 - 1,500	2,500 - 5,000
C	Soft rock and Very dense Soil	poorly-cemented coarse-grained to fine-grained sedimentary rock to dense Early to mid Pleistocene or older granular sediment	350 - 750	1,200 - 2,500
D	Stiff Soil	Mid to Late Pleistocene granular sediment or properly Enginered Fill (post 1985)	200 - 350	600 - 1,200
E	Soft Soil	Holocene granular sediment, pre-1985 artificial fill, includes some Late Quaternary muds, sands, gravels, silts and mud. Significant amplification of shaking by these soils is generally expected.	< 200	< 600
F	Unstable Soil	Includes water-saturated mud and undocumented or pre-1950 artificial fill. The strongest amplification of shaking due is expected for this soil type.	requires site specific measurement	requires site specific measurement

Two basic types of energy are generated when an acoustic source strikes the surface of the ground: (1) body waves and (2) surface waves.

Body waves are non-dispersive; the velocity of propagation is a function of the engineering properties of the soil and rock through which the waves are traveling (Figure 3.10). Body waves are comprised of compressional (P-waves or Vp) and shear-waves (S-

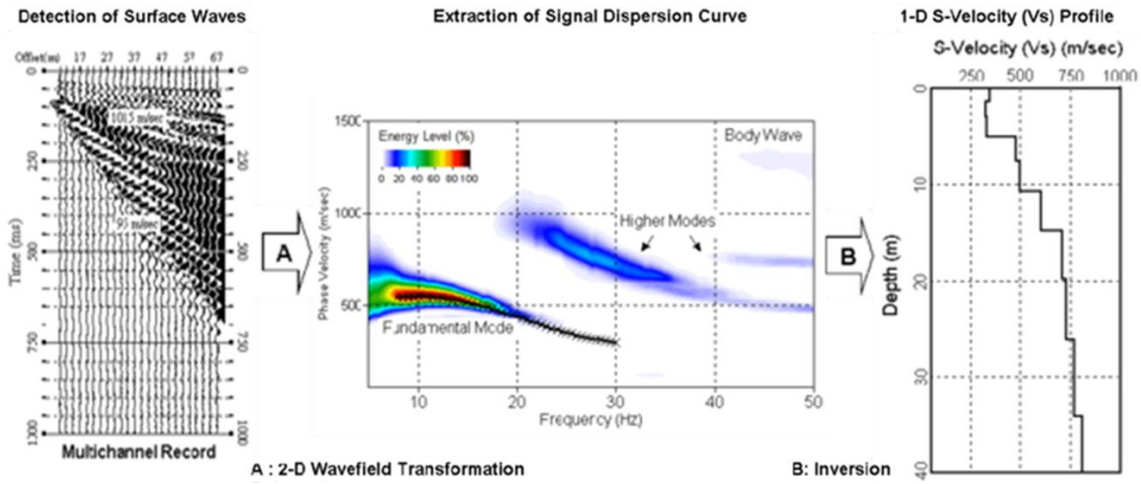

Figure 3.9. Overview of MASW data processing.
Images from left to right: (1) Extraction of a trace from the raw data; (2) Creation of a phase velocity vs frequency profile (dispersion curve); (3) Generation of a 1-D vertical shear wave velocity profile (depth vs. shear wave velocity).

waves or Vs). P-waves are compressional strain waves wherein particle motion is parallel to the direction of wave travel. S-waves, in contrast, propagate by a strain in the direction perpendicular to the wave direction of wave travel.

Surface waves are comprised of Love and Rayleigh waves, both of which are dispersive. Rayleigh wave particle motion is retrograde elliptical and decreases exponentially with depth; hence they are referred to as surface waves (Anderson, 2004). Love wave particle motion is horizontal and perpendicular to the direction of wave propagation.

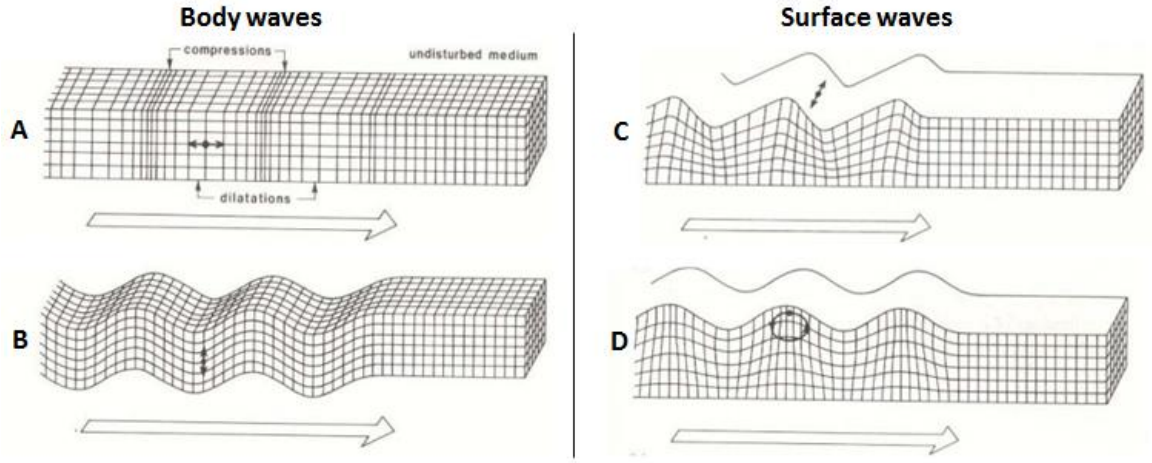

Figure 3.10. Particle motion of different waves. (**A**) Compressional (P) waves, (**B**) Shear (S) waves, (**C**) Love waves, and (**D**) Rayleigh waves (Anderson, 2004).

For MASW surveys we are only interested in the Rayleigh wave data. As such we ignore recorded body wave energy.

In a homogenous medium, phase velocity of the Rayleigh waves are consistent and can be determined using the following Equation 3.1:

$$V_R^6 - 8\beta^2 V_R^4 + (24 - 16\beta^2/\alpha^2)\beta^4 V_R^2 + 16(\beta^2/\alpha^2 - 1)\beta^6 = 0 \quad [3.1]$$

where V_R is the Rayleigh wave velocity within the uniform medium, β is the shear-wave velocity within the uniform medium, and α is the compressional wave velocity within the uniform medium.

For the purpose of MASW, Equation 3.1 is reduced to $V_R = 0.919\,\beta$ [3.6] because V_R is relatively insensitive to changes in α. To convert Equation 3.1 to the relation between V_R and β, the relation between α and β needs to be determined. This

determination is made using the Scalar wave equation, which explains the relation between compressed wave, shear-wave, density, bulk modulus, and shear modulus.

The Scalar wave equation is:

$$\boldsymbol{\alpha} = \sqrt{(\boldsymbol{\lambda} + \mathbf{2}\boldsymbol{\mu}/\boldsymbol{\rho})}$$

$$\boldsymbol{\beta} = \sqrt{(\boldsymbol{\mu}/\boldsymbol{\rho})}$$

where $\boldsymbol{\alpha}$ is the compressional wave velocity, $\boldsymbol{\beta}$ is the shear-wave velocity, $\boldsymbol{\rho}$ is the density of the material, $\boldsymbol{\lambda}$ is bulk modulus and $\boldsymbol{\mu}$ is shear modulus.

Hooke's Law summarizes the relationship between bulk modulus, shear modulus and Poisson's Ratio:

$$\boldsymbol{\sigma} = \boldsymbol{\lambda}/\mathbf{2}(\boldsymbol{\lambda} + \boldsymbol{\mu})$$

where $\boldsymbol{\sigma}$ is Poisson's Ratio.

By combining equations [3.2], [3.3] and [3.4] we can get the relation of $\boldsymbol{\alpha}$ and $\boldsymbol{\beta}$ as:

$$\frac{\boldsymbol{\beta}}{\boldsymbol{\alpha}} = \sqrt{(\mathbf{0.5} - \boldsymbol{\sigma})/(\mathbf{1} - \boldsymbol{\sigma})}$$

The values of Poisson's Ratio for many materials are close to the initial recommendation of 0.25 by Poisson, and later analyzed to be closer to 0.33 by Guillame

Wertheim (Gercek, 2007), so Equation 3.5 should equal to 0.33. Using this relation of the shear-wave and compressional wave in Equation 3.1 will result in Equation 3.6:

$$\mathbf{V_R = 0.919\,\beta} \qquad [3.6]$$

Using this final Equation 3.6 we can now compare the given Rayleigh ($\mathbf{V_R}$) wave and calculate the shear-wave (**β)** to determine the classification of the given material (Li, 2018).

3.2.2. Acquisition and Survey. To collect the MASW data at Lake Chesterfield, an array of geophones were placed at uniform intervals (2.5 or 5 ft.) along linear traverses (Figure 3.11). MASW data were acquired at a total of 11 locations (Figure 3.4). Only 5 MASW profiles (MASW locations: 2, 3, 8, 9 and 11) were made available to the author of this thesis.

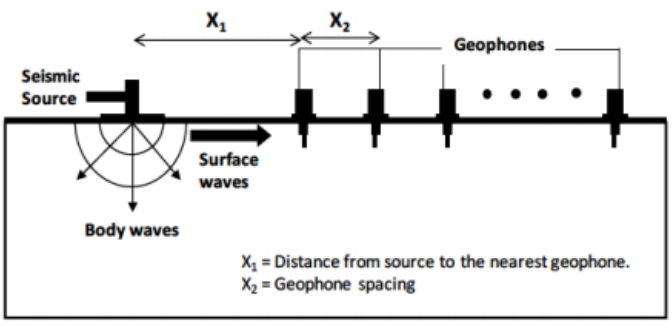

Figure 3.11. Typical geometry used for MASW data acquisition.

A 20 lb. sledge hammer was used as the seismic source. Offsets (X_1) were either 25 ft. or 15 ft. Data were recorded using twenty-four 4.5Hz geophones spaced at an intervals (X_2) of either 5 ft. or 2.5 ft. Changes to geophone spacing and offset will alter

the depth of investigation and quality of the data. Shorter geophone spacing and offset generally produces good quality data at shallower depths. Larger geophone spacings and offsets will generally increase the depth of investigation.

Seismic data were compiled and analyzed using Surfseis 4, a software developed by the Kansas Geological Survey, to create a final 1-D shear wave velocity profile for each traverse and compared to the ERT data acquired.

3.2.3. MASW Data Interpretation. A total of five MASW profiles were acquired, MASW profiles 2, 3, 8, 9, and 11. The 1-D shear-wave velocity profile (herein referred to as MASW profile 3) generated for MASW location 3 is shown in Figure 3.12. This 1-D shear-wave velocity profile ties the ERT profile shown in Figure 3.5 (at station 349 ft.).

The interpreted top of rock at station 349 ft. on the ERT profile shown in Figure 3.5 is at a depth of approximately 5 ft. The zone interpreted as highly weathered rock extends from a depth of approximately 10 ft. to a depth of approximately 20 ft. The top of soft rock (at best) on the corresponding MASW 1-D shear-wave velocity profile Figure 3.12 is at a depth of approximately 1.5 ft. Based on shear-wave velocity only, the material at depths between 6 and 16.5 ft. would be classified as soil (according to NEHRP classification system (Table 3.1)). According to the NEHRP classification system, the earth material at depths greater than 38 feet would be classified as rock.

It is interesting to note that the engineers who designed the dam identified the top of the soft rock (consistent with top-of-rock on the ERT data) as top-of-rock. In contrast, the company that did the grouting referred to the highly weathered rock (as per ERT interpretation) as residual soil.

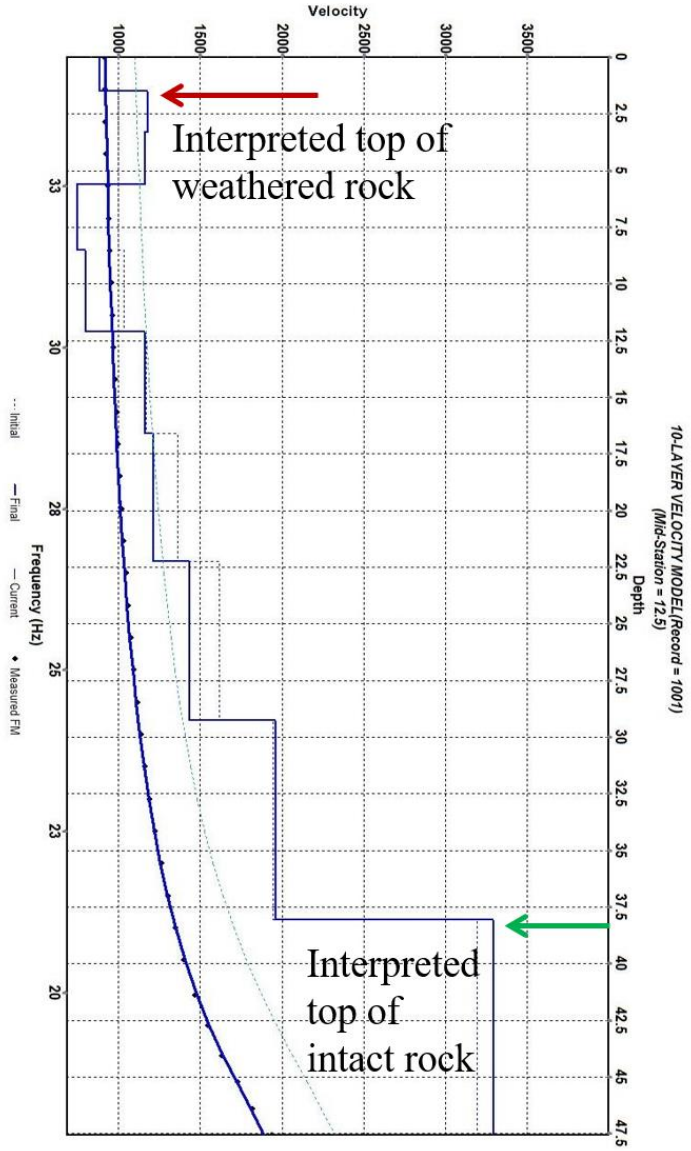

Figure 3.12. 1-D 10-layer model of shear-wave velocity profile of MASW profile 3.

When comparing the MASW and ERT data sets, the depths to weathered and intact rock are reasonably consistent with each other. This gives us confidence in our data and interpretation. It is not unreasonable to expect discrepancies (as shown in this example, Figure 3.5 and 3.12) between the MASW and ERT estimates of depth to top-of-rock. Discrepancies between the MASW and ERT estimates can be attributed to a couple

of factors. First, the MASW top of weathered rock is picked based on acoustic velocity, whereas the ERT top of weathered rock is picked based on resistivity. Second, the vertical resolution on the ERT data is higher than on the MASW 1-D shear-wave velocity profiles.

Interpretations of both the MASW and ERT data supports the interpretation that rock between elevations 620-640 ft. is highly weathered in places and that the dam was constructed, in places, on highly weathered rock. Further, the interpretation of the ERT and MASW data supports the thesis that clay liner breaches in places due to the weight of the water when the dam is filled and that waters that flow into the breaches ultimately flow to the north beneath the dam through weak rock.

3.3. SPONTANEOUS POTENTIAL (SP)

Spontaneous Potential (SP), also known as Self Potential, is a tool used to map the naturally occurring electrical potential, in millivolts (mV), of the earth between a fixed reference (base station) electrode and a lead electrode moved to different locations (roving station) in the survey area (Figure 3.13). Electrical potential is created within in the subsurface due to a few factors including the flow of water (electrokinetic potential), and diffusion potential.

3.3.1. Basic Principles of SP. The electrokinetic potential, as used in the present survey, is produced when water flows into, through or out of a medium. Water flowing into the subsurface (infiltration) is generally characterized by negative SP values (Figure 3.14). In contrast, water flowing out of the ground (e.g. spring) is generally characterized by positive SP values.

3.3.2. Acquisition and Survey. The electrodes used in the survey were non-polarizing $Cu/CuSO_4$ electrodes also known as porous pots. A fixed reference base electrode was placed on the western bank of the lake below the tennis court (Figure 3.4 and 3.15). A second lead electrode was then placed at multiple locations along the existing ERT traverses and measurements were taken every 5-10 ft., and stored using the same AGI Supersting, R8 that was used for the ERT data collection. For quality control purposes, the SP measurements were taken up to 3 times at each station location. When the data error value varied less than 2%, the value was recorded.

3.3.3. SP Data Interpretation. The SP results, as seen in Figure 3.15, show two main areas of interest. The first is Location 1, which was located 180 ft. from the start on traverses 6-8. The second is Location 2, which was located along the northeast edge of the lake.

These two areas are characterized (mostly) by negative (blue) SP values. The areas of negative SP values correlate well with areas of low resistivity on the ERT profiles, suggesting that water is infiltrating the subsurface at these locations. As these negative zones are not located above the interpreted solution-widened joints on the ERT data. Expectations then, are that the seeping waters flow to the north through the zone of weathered rock and beneath the dam through the interpreted seepage pathways (Figure 3.8), and not down through the solution-widened joints (Figure 3.7).

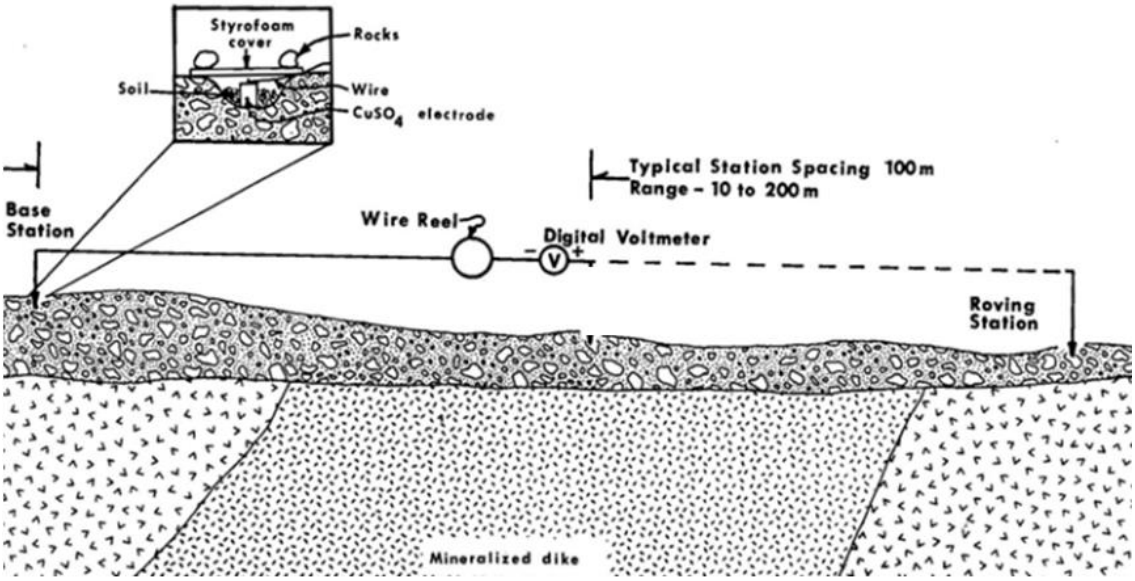

Figure 3.13. Schematic set-up and collection of SP data. (Corry, 1982).

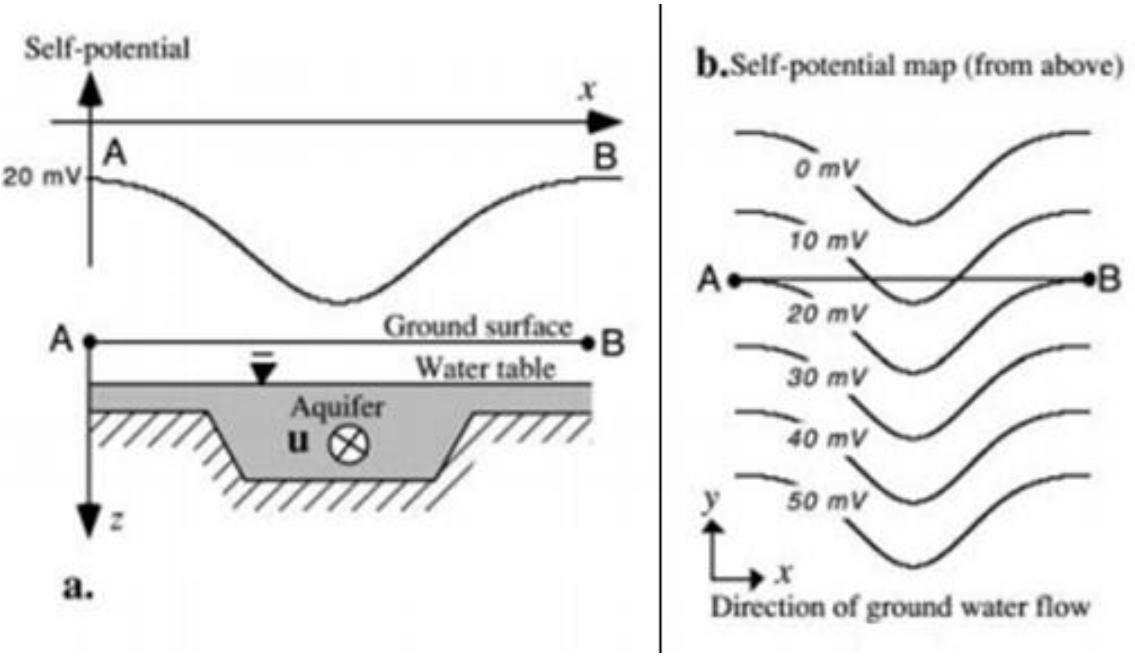

Figure 3.14. (a) Induced negative electrokinetic potential associated with the flow of water in the ground. (b) SP map in plane view (Revil, 2107).

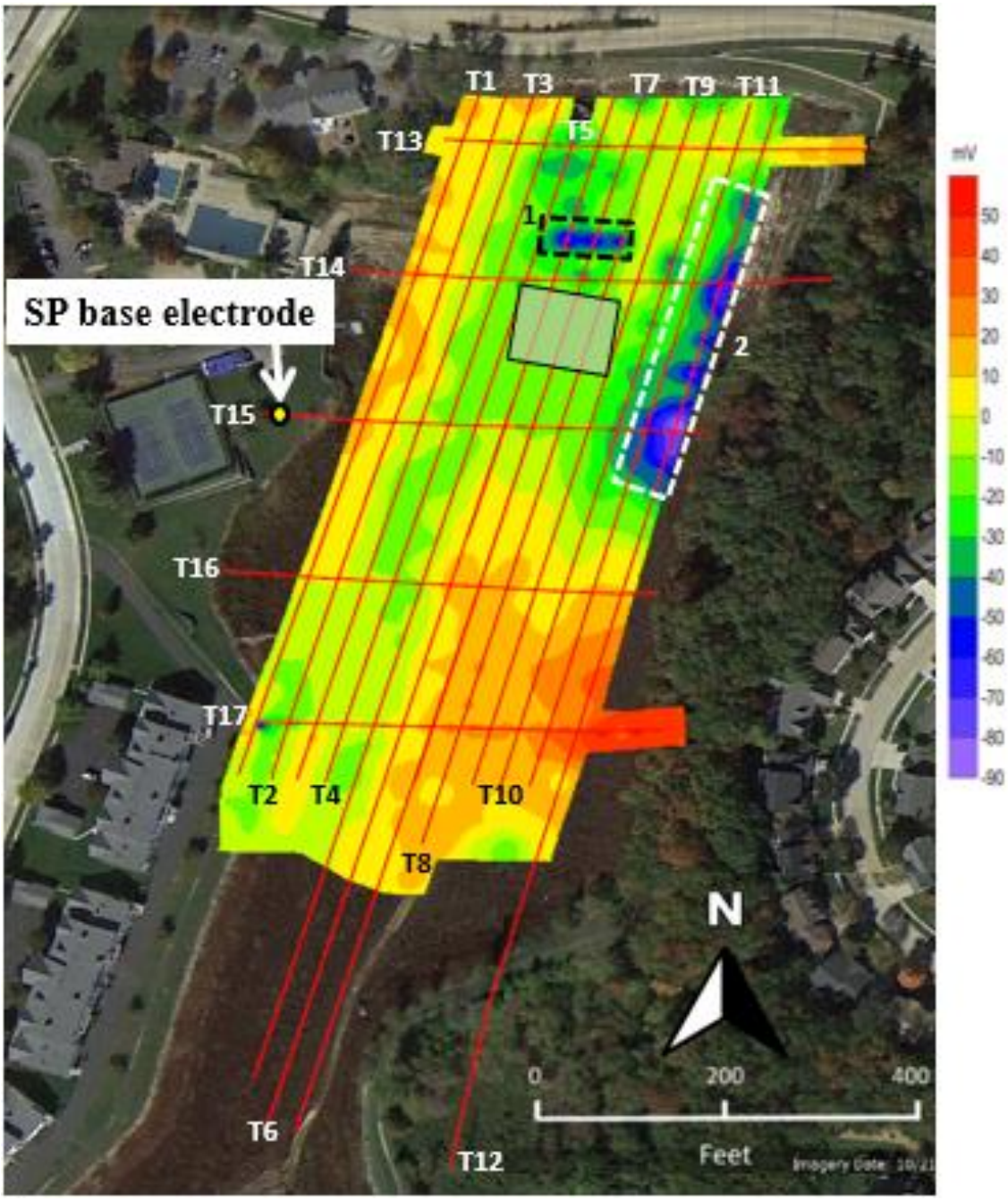

Figure 3.15. Contoured SP data overlaid on Lake Chesterfield. Red lines indicate the location of the ERT traverses (T1-17) along which the SP data were acquired. Two prominent negative SP anomalies are highlighted (1 and 2). These anomalies are shown in blue/purple. Data couldn't be acquired in grey shaded area due to the presence ponded water (Anderson, 2018).

4. CONCLUSIONS

The purpose of the study was to 1) map variable depth to top of bedrock, 2) determine the variable quality of the shallow bedrock, 3) identify any significant karst features beneath the lake, and 4) identify any probable seepage pathways.

4.1. DEPTH TO TOP OF BEDROCK

The variable top of bedrock was estimated using the ERT and MASW datasets. Across the northern section of Lake Chesterfield there is a distinctive depression in the depth to top of bedrock (Figure 3.6) as evident from the ERT data. This depression is the location of the 2004 sinkhole and subsequent remediation efforts.

The rest of the northern section of Lake Chesterfield, the top of bedrock is mostly consistent at depths ranging from 5-10 ft. beneath the lake bed.

4.2. QUALITY OF BEDROCK

The quality of the bedrock in the northern section of Lake Chesterfield varies significantly, and can be divided into three sections on the basis of resistivity and shear-wave velocity: 1) Intact limestone is characterized by resistivities greater than 250 Ohm-m, and shear-wave velocities greater than 2500 ft/sec. Based on the shear-wave velocities alone in accordance with the NEHRP classification system, the intact limestone would be classified as rock. The intact limestone can be seen typically at elevations lower than 620 ft.

2) Weathered limestone, characterized by resistivities between 75 and 250 Ohm-m, and shear-wave velocities between 1200 and 2500 ft/sec. Based on the shear-wave velocities alone in accordance with the NEHRP classification system, the weathered limestone would be classified as soft rock or dense soil. This weathered limestone can typically be seen between elevations 630-645 ft.

3) Highly weathered limestone, characterized by resistivities lower than 75 Ohm-m, and shear-wave velocities lower than 1200 ft/sec. Based on the shear-wave velocities alone in accordance with the NEHRP classification system, the highly weathered limestone would be classified as stiff soil. This highly weathered limestone can typically be seen between elevations 620-640 ft.

4.3. KARST FEATURES

Shallow rock in the study area is dissected by solution-widened joints and is extensively weathered. Some of the more prominent solution-widened joints appear to extend to depths below the maximum depth of coverage on the ERT profiles. It is possible that waters seep vertically into the subsurface along these joints. In the author's opinion, it is more likely that the karst features pinch out at depth and do not serve as vertical conduits. If they did, the SP anomalies should be situated above these same solution-widened joints.

4.4. SEEPAGE PATHWAYS

Seepage from Lake Chesterfield could occur in three ways: 1) beneath the dam, 2) vertically, and 3) laterally.

4.4.1. Seepage Beneath the Dam. Three zones of low resistivity are identified on Figure 3.7. These zones are interpreted as probable seepage pathways beneath the dam. The idea that water is seeping to the north is backed-up by the emergence of the dye near Lewis Spring during the dye test in 2004, and not anywhere else.

4.4.2. Seepage Vertically. Interpreted solution-widened joints can be seen extending vertically on several the ERT profiles. The most prominent on traverses 5 at station 320 ft., 6 at station 400 ft., 11 at station 400 ft. and 12 at station 440 ft (Figure 3.7 and Appendix A). It is possible that waters seep vertically into the subsurface along these joints. In the author's opinion, it is more likely that the karst features pinch out at depth and do not serve as vertical conduits. If they did, the SP anomalies should be situated above these same solution-widened joints.

4.4.3. Seepage Laterally. In the author's opinion, waters that seep into the subsurface flow northward through the variably weathered rock and beneath the dam.

5. RECOMMENDATIONS

The current owners of Lake Chesterfield, LCHOA, stated they have spent close to a million dollars over the past 10 years trying to stop the leaking of the lake through the addition of clay liners. As the mitigation efforts performed up to this point have not yet solved the leaking issues, there are two options that could be potential solutions for the leak.

The first is to grout the lake along interpreted flow paths. Grouting in the lake has already been utilized on numerous occasions, specifically when small sinkholes formed around the lake. Although the grouting has been effective in stopping the flow of water in the areas where the work has been performed, new flow paths have opened over time, as evident in the geophysical data of this current survey. The most effective location for potential grouting to stem the flow of water beneath the dam would need to be along the three prominent low resistivity zones identified on ERT traverse 13 at stations 120 ft., 260 ft. and 340 ft. Targeted grouting along this traverse could help stem the flow of water.

The second option for the LCHOA is to utilize reinforced rubber linings. The lake is currently lined by clay liners. These clay liners are being compromised by the hydrostatic pressures that flushes them (gradually to catastrophically) into the underlying variably weathered rock. Utilizing a reinforced polyethylene (RPE) liner, ethylene propylene diene monomer (EPDM) liner, or polyvinyl chloride (PVC) liner would be a better long-term solution.

APPENDIX A.

ERT PROFILES, NNE-SSW 1-12 AND W-E 13-15 WITH INTERPRETATIONS

ERT Profile 1

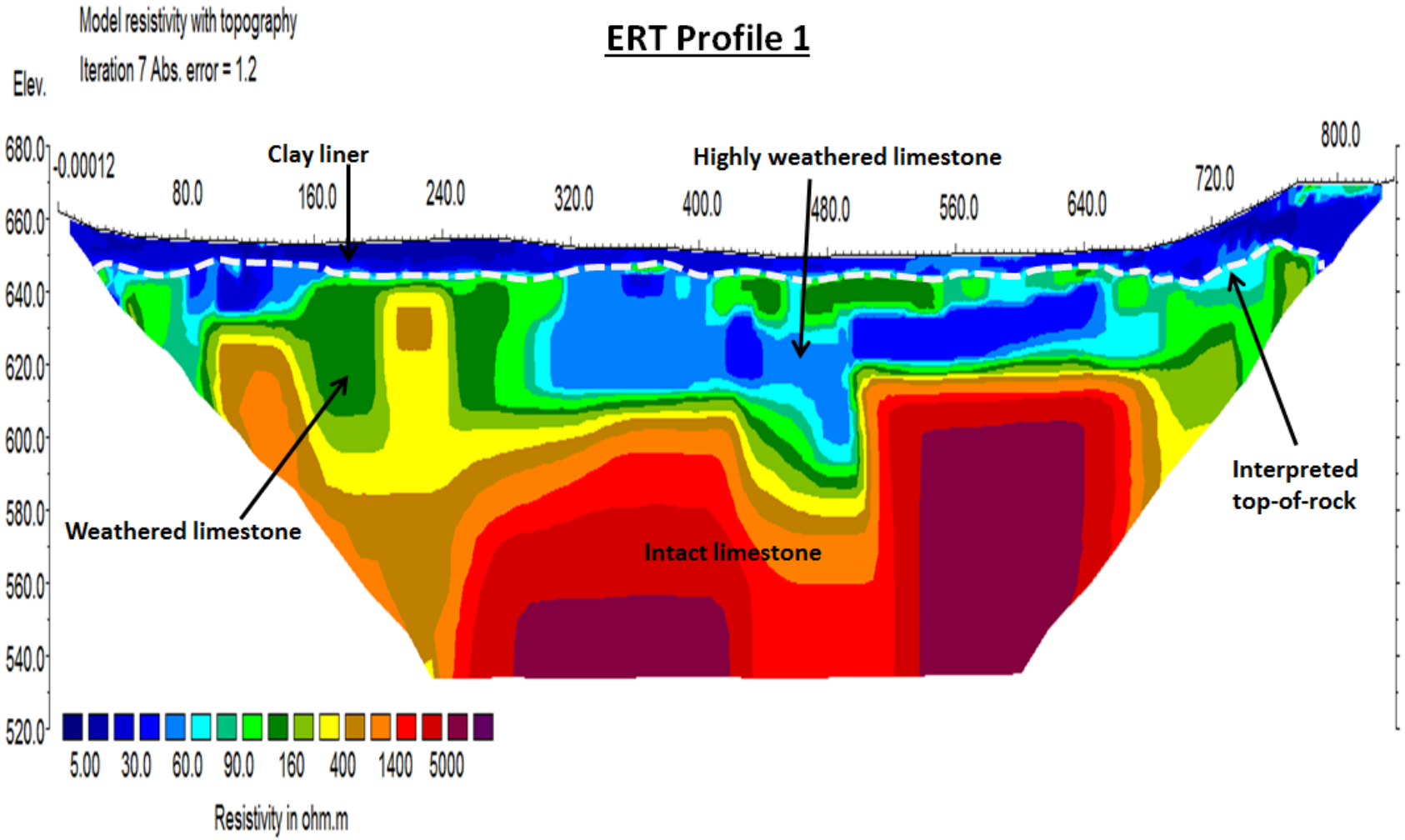

ERT Profile 2

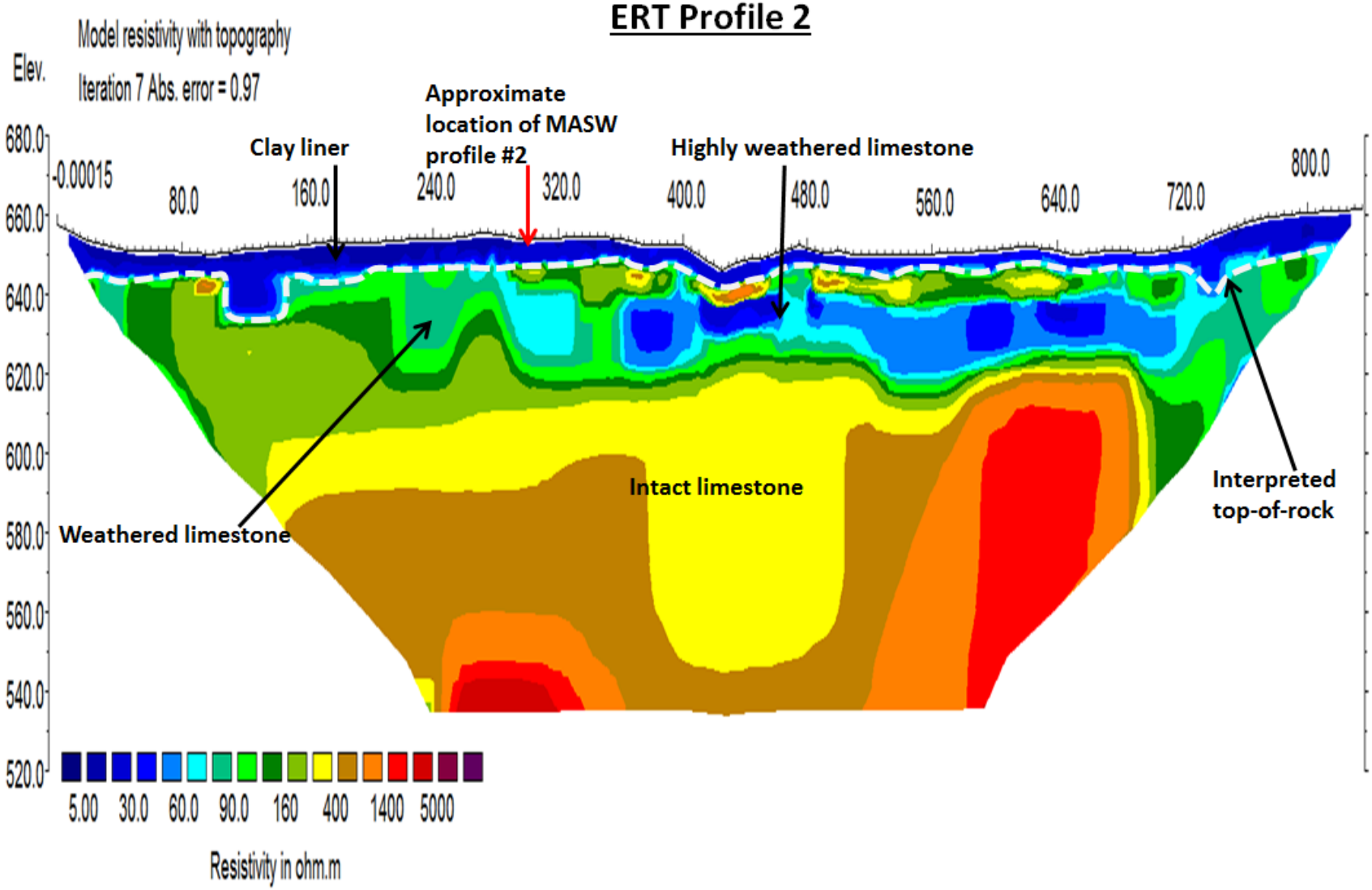

Profile 3

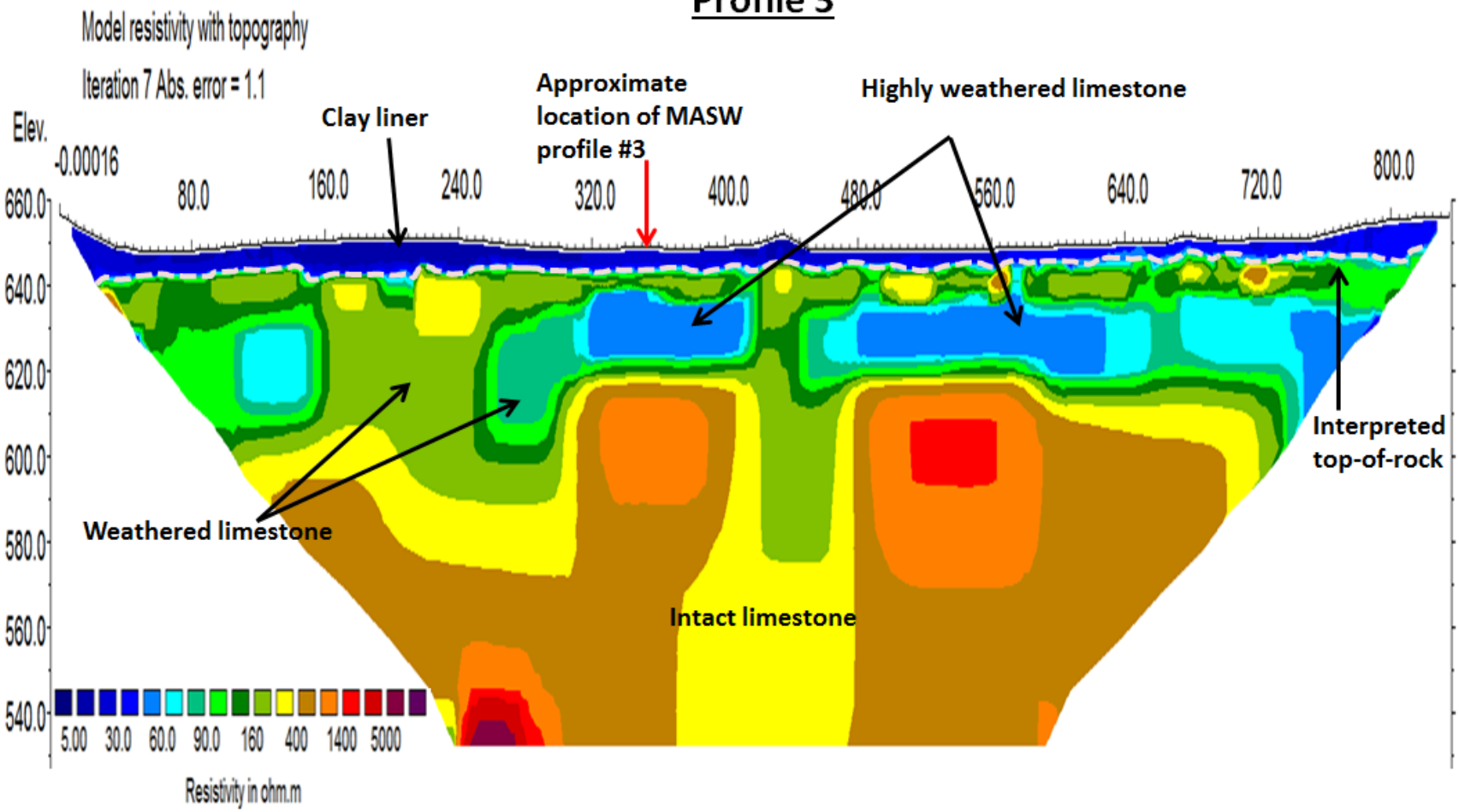
Model resistivity with topography
Iteration 7 Abs. error = 1.1
Elev.
-0.00016
80.0
160.0
240.0
320.0
400.0
480.0
560.0
640.0
720.0
800.0
660.0
640.0
620.0
600.0
580.0
560.0
540.0
Clay liner
Approximate location of MASW profile #3
Highly weathered limestone
Interpreted top-of-rock
Weathered limestone
Intact limestone
5.00 30.0 60.0 90.0 160 400 1400 5000
Resistivity in ohm.m

ERT Profile 4

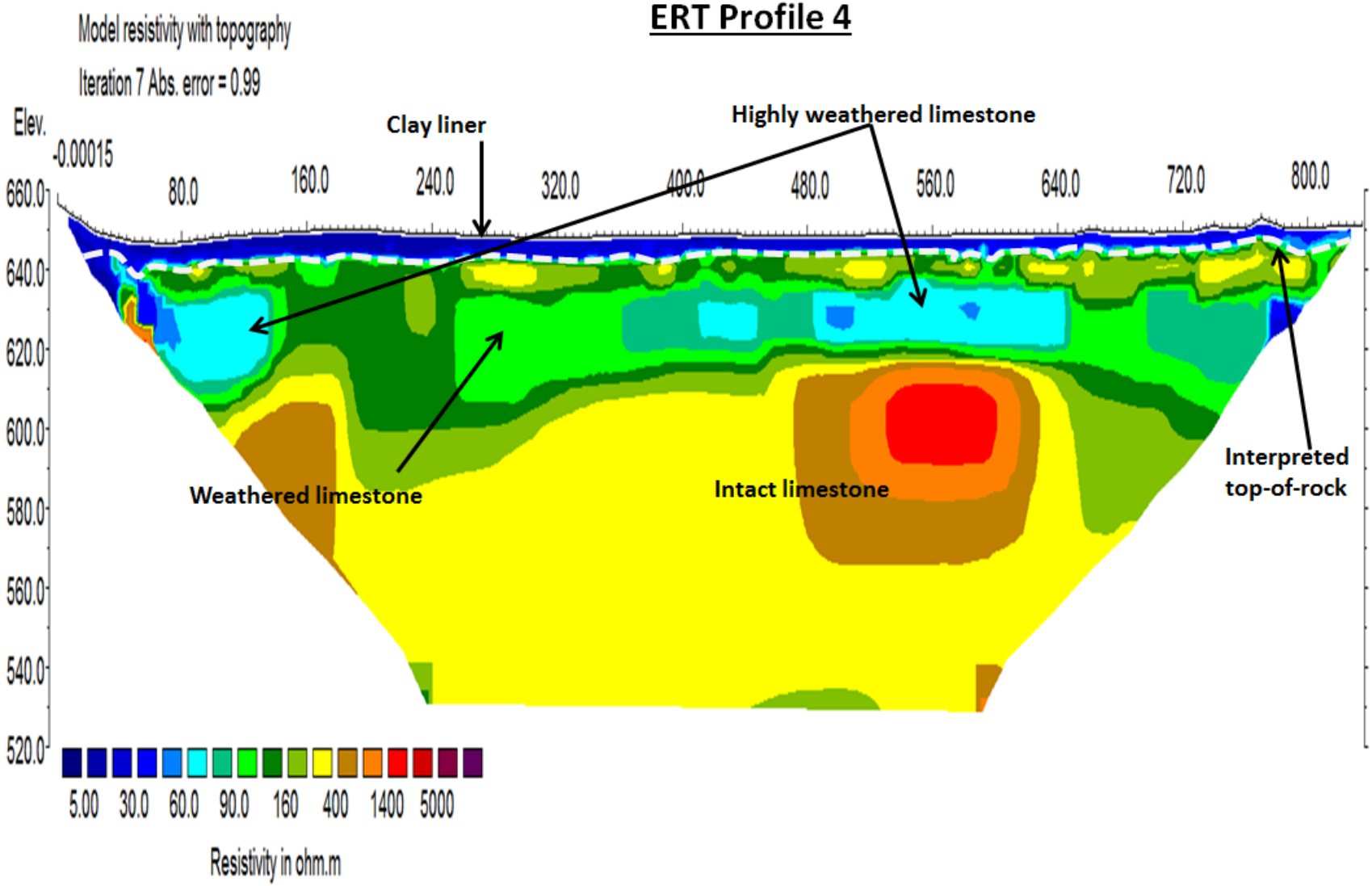

ERT Profile 5

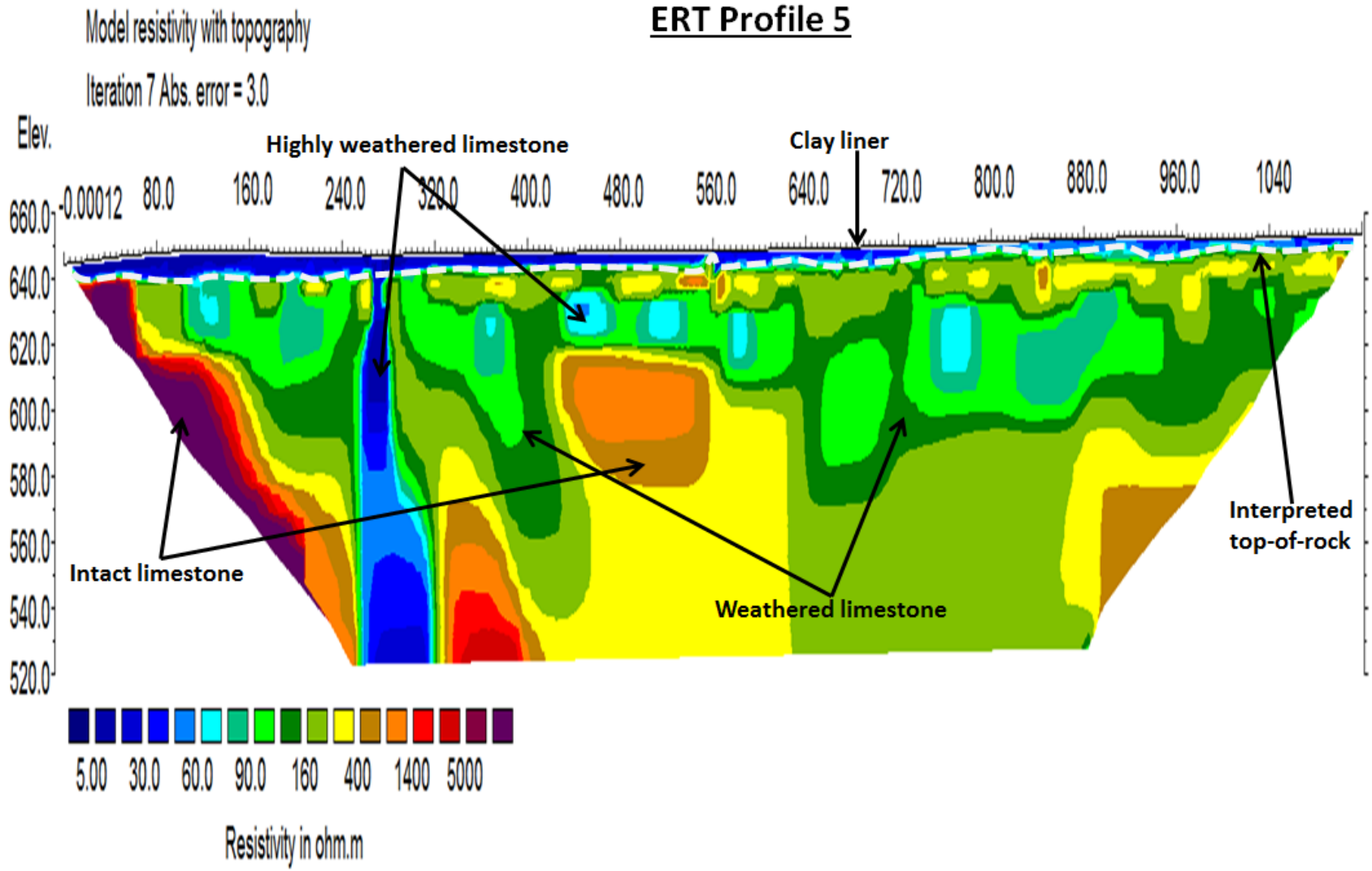

ERT Profile 6

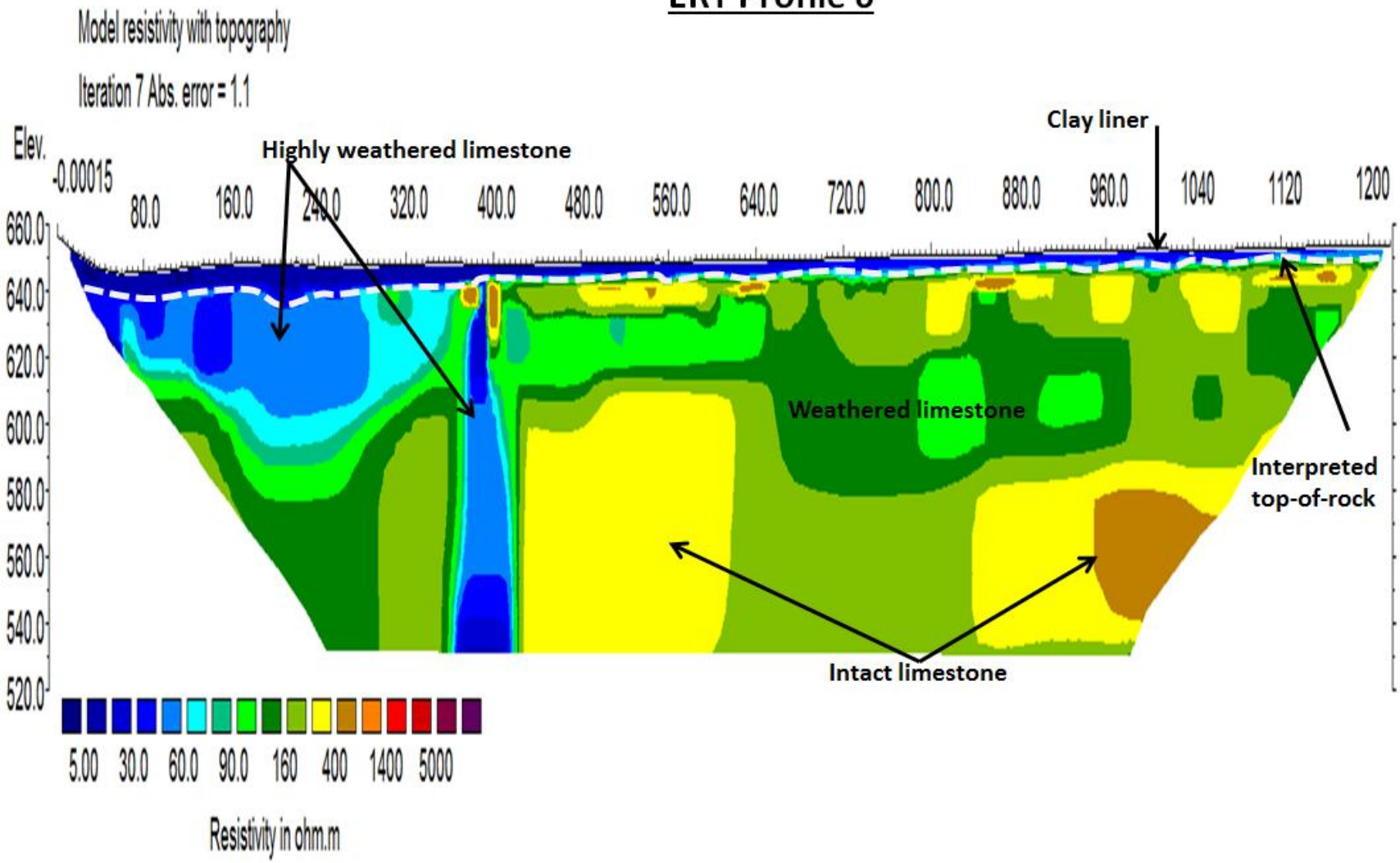

ERT Profile 7

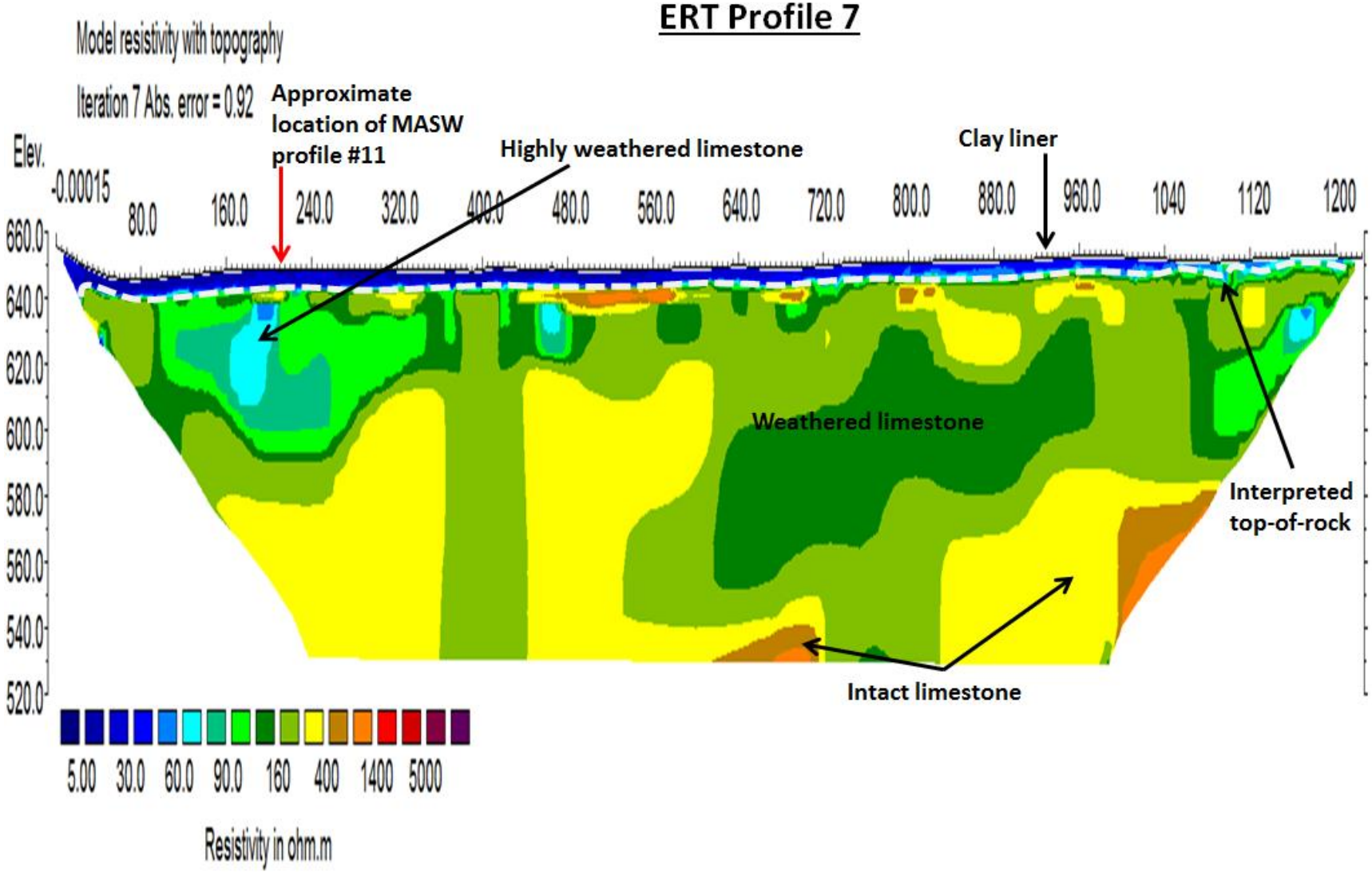

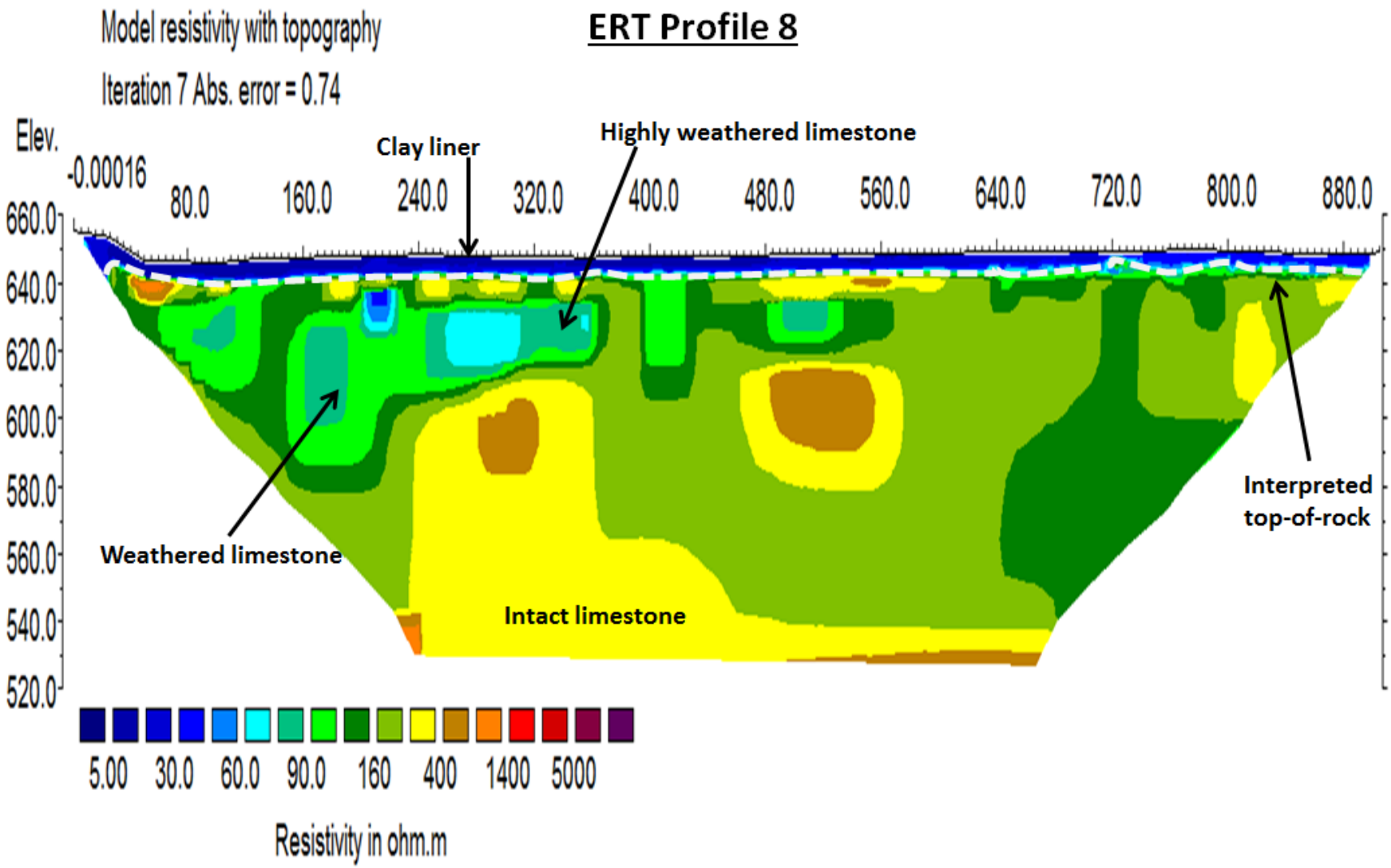
ERT Profile 8
Model resistivity with topography
Iteration 7 Abs. error = 0.74
Elev.
-0.00016
80.0
160.0
240.0
320.0
400.0
480.0
560.0
640.0
720.0
800.0
880.0
660.0
640.0
620.0
600.0
580.0
560.0
540.0
520.0
Clay liner
Highly weathered limestone
Weathered limestone
Intact limestone
Interpreted top-of-rock
5.00
30.0
60.0
90.0
160
400
1400
5000
Resistivity in ohm.m

ERT Profile 9

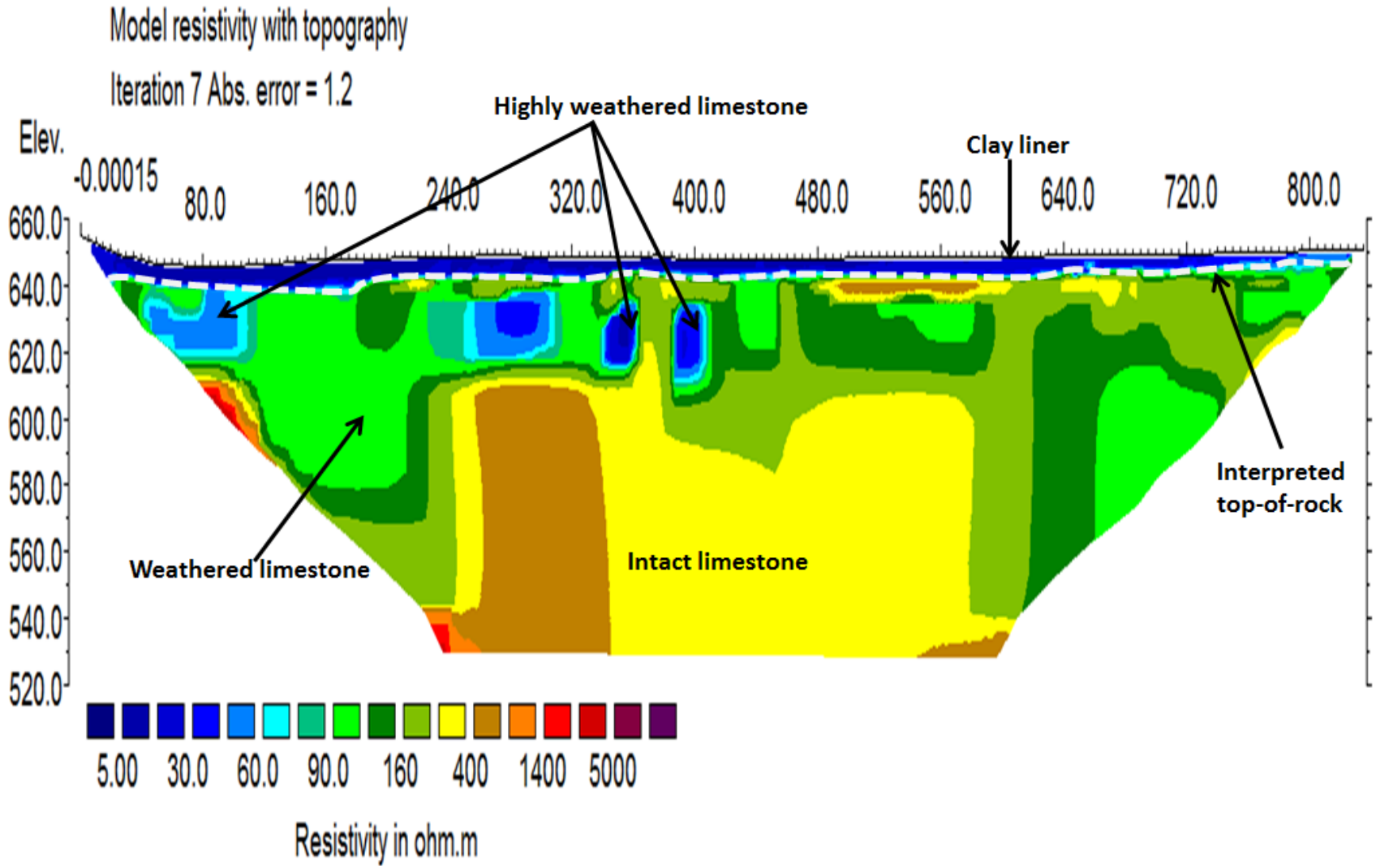

ERT Profile 10

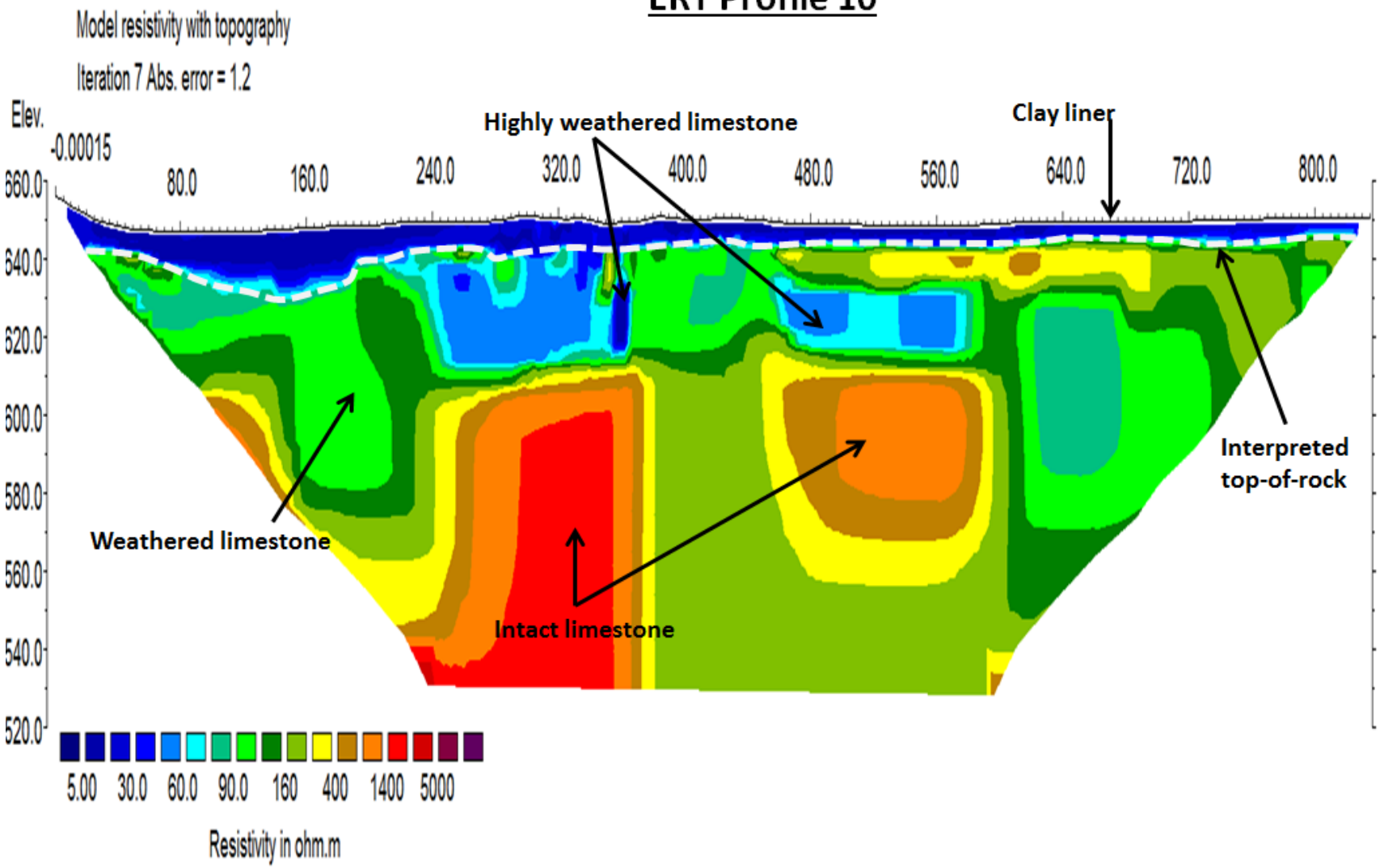

ERT Profile 11

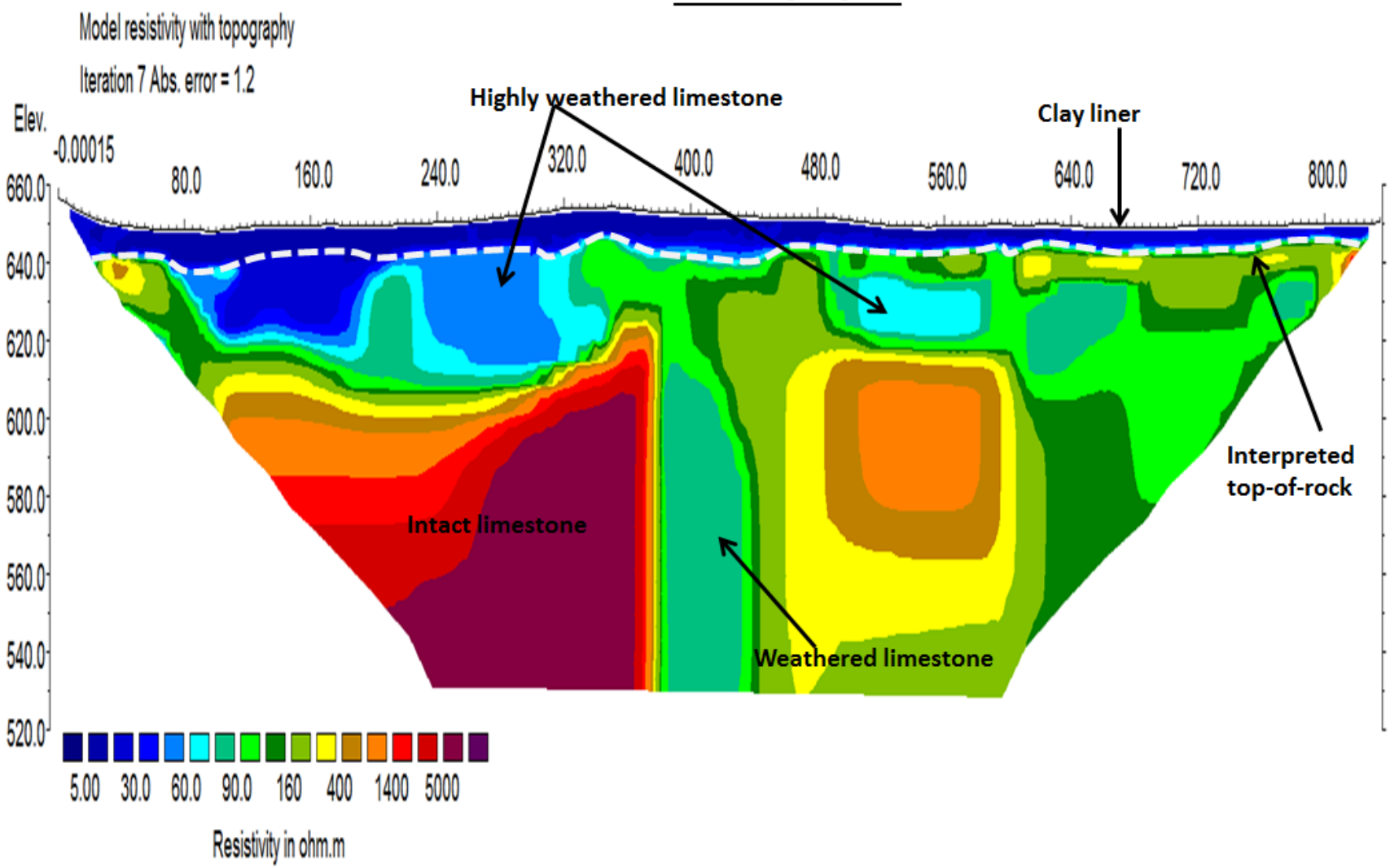

ERT Profile 12

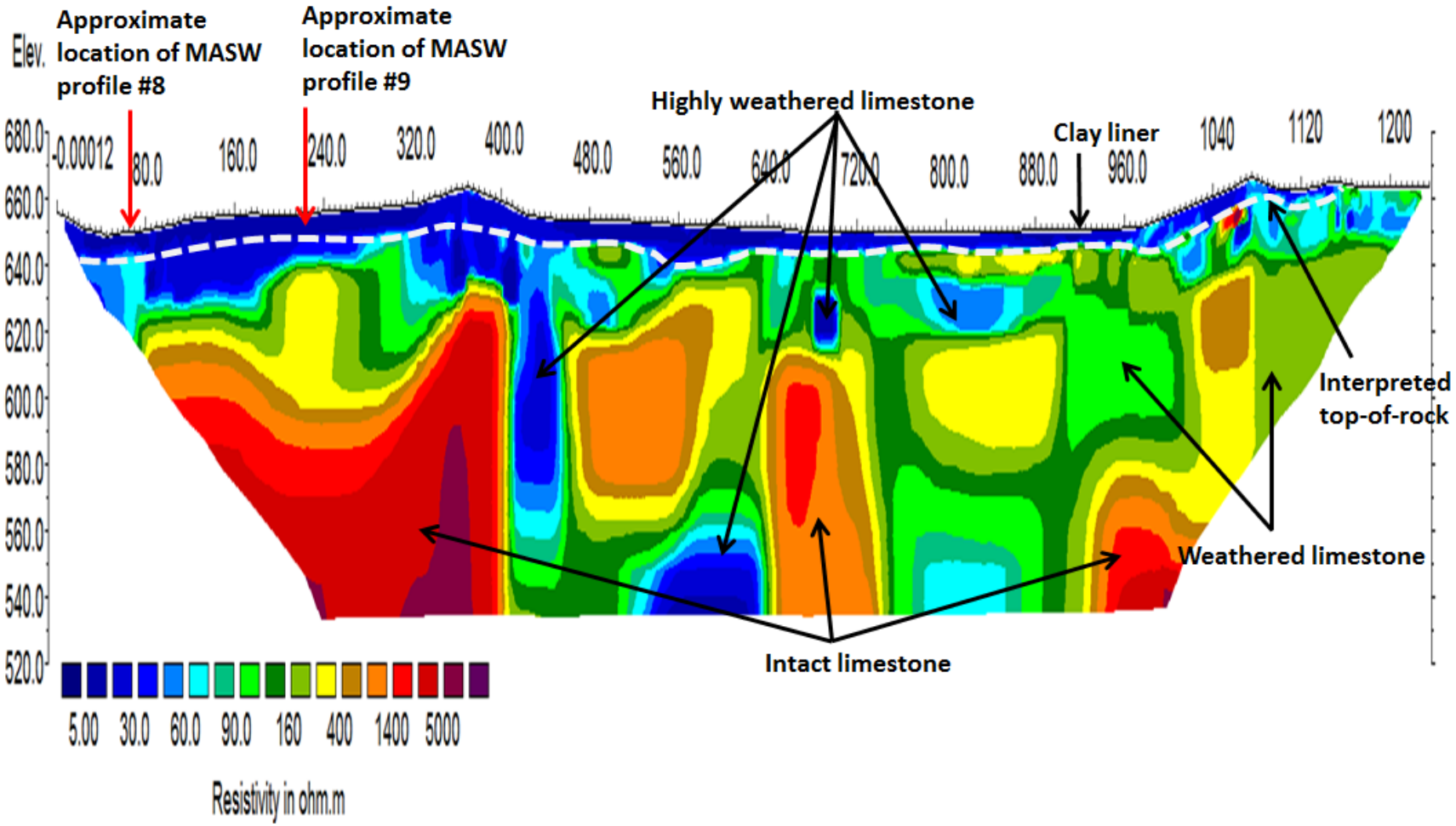

ERT Profile 13

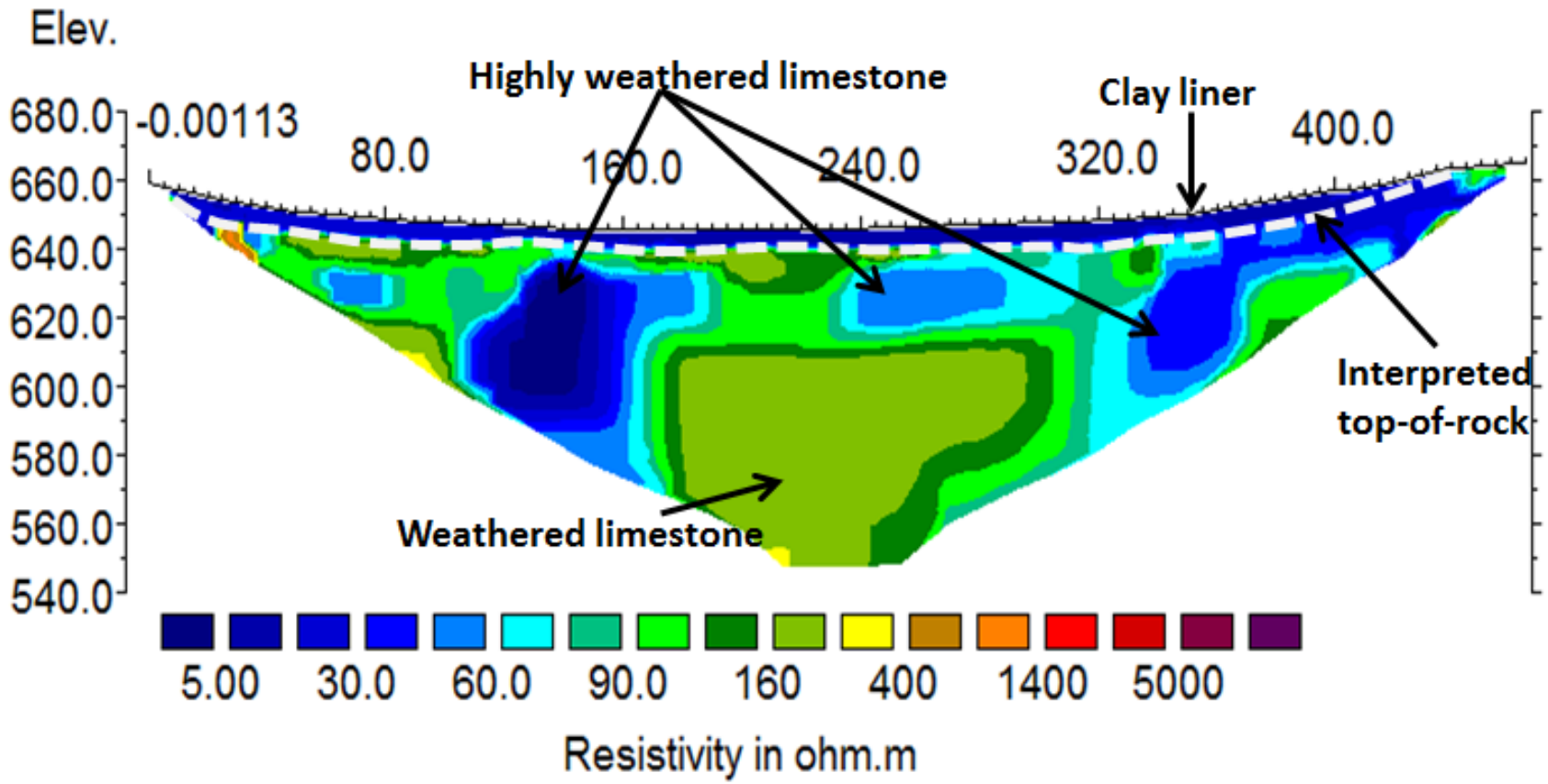

ERT Profile 14

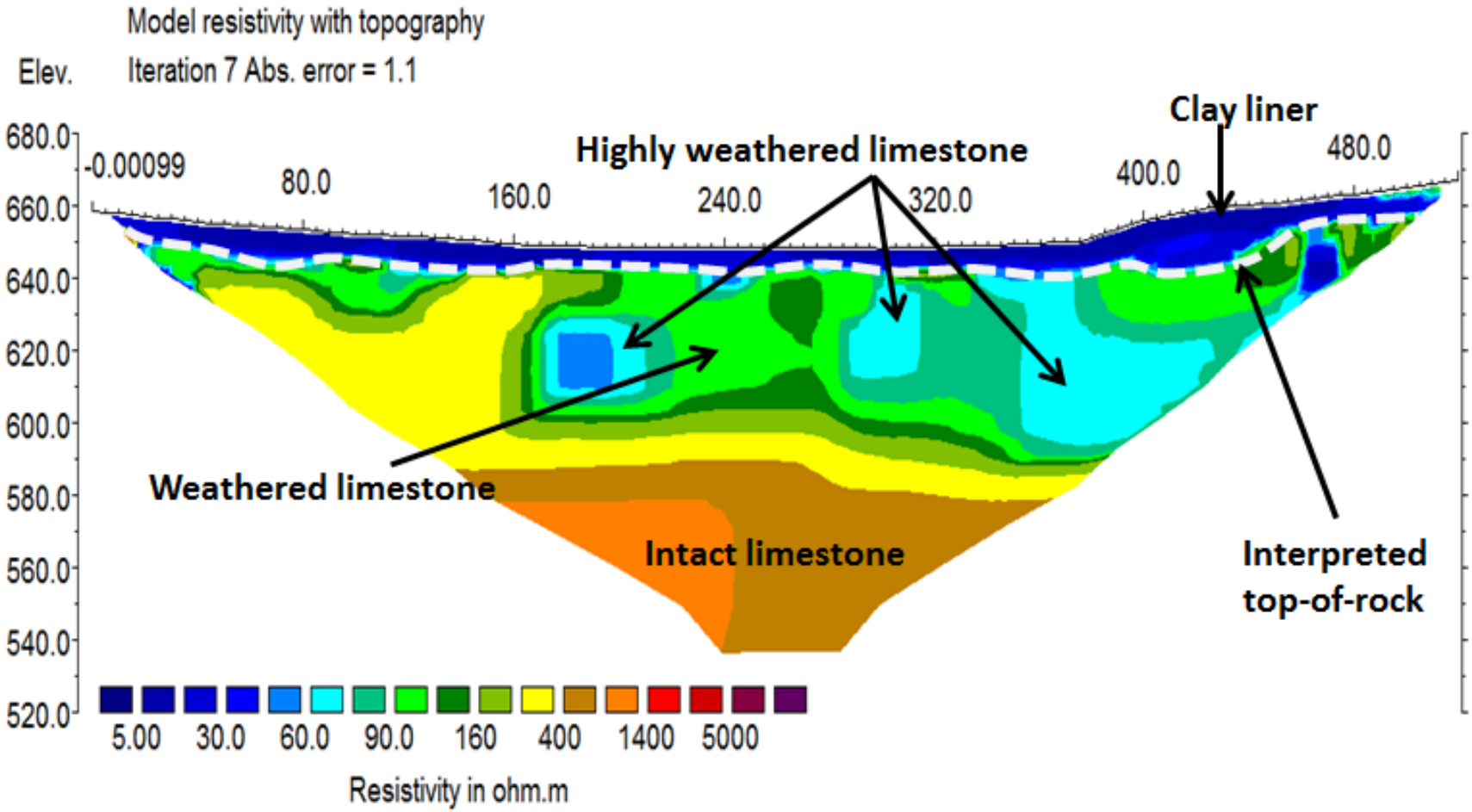

ERT Profile 15

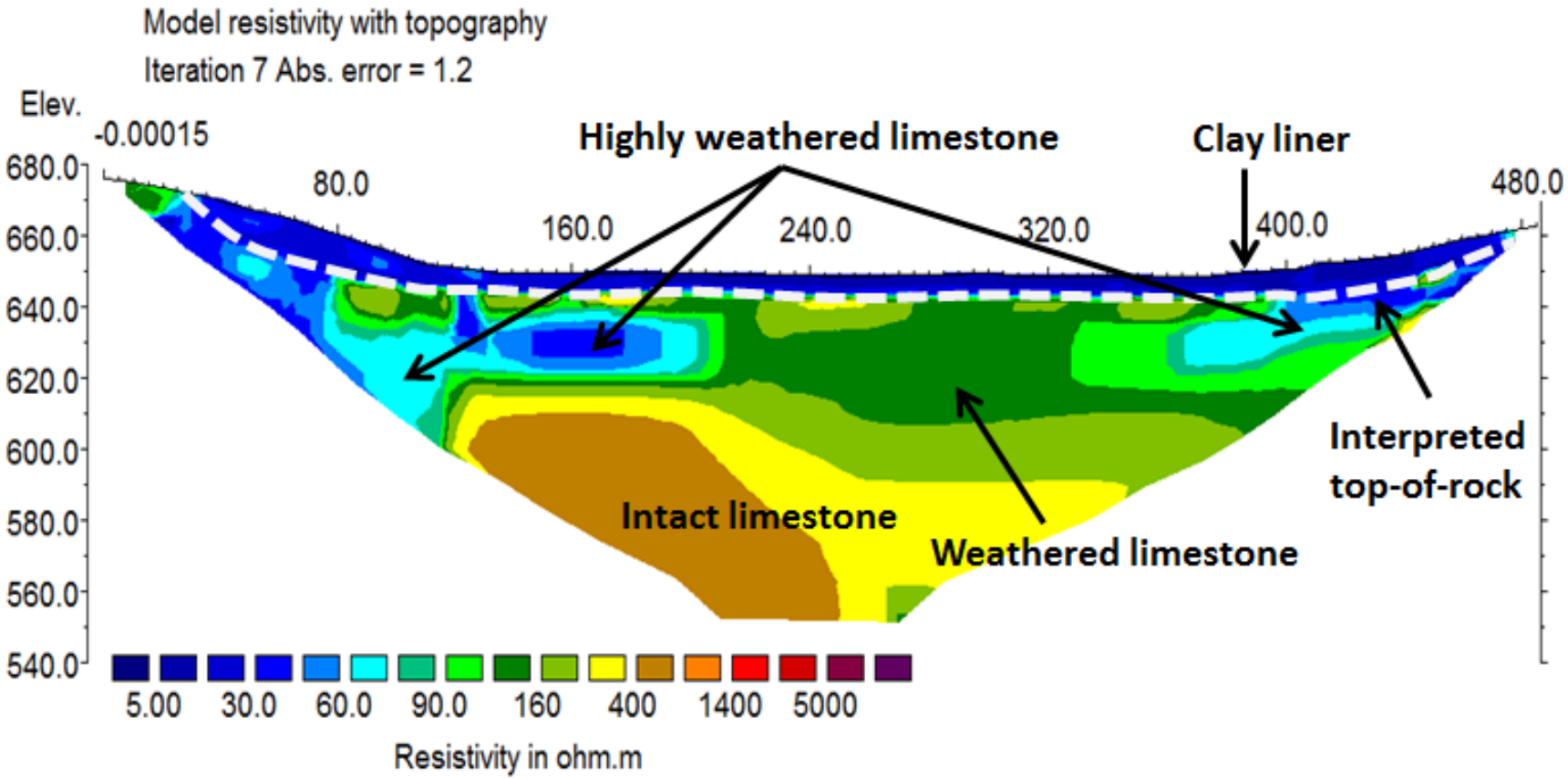

APPENDIX B.

MASW PROFILES 2, 3 8, 9, AND 11 WITH INTERPRETATIONS

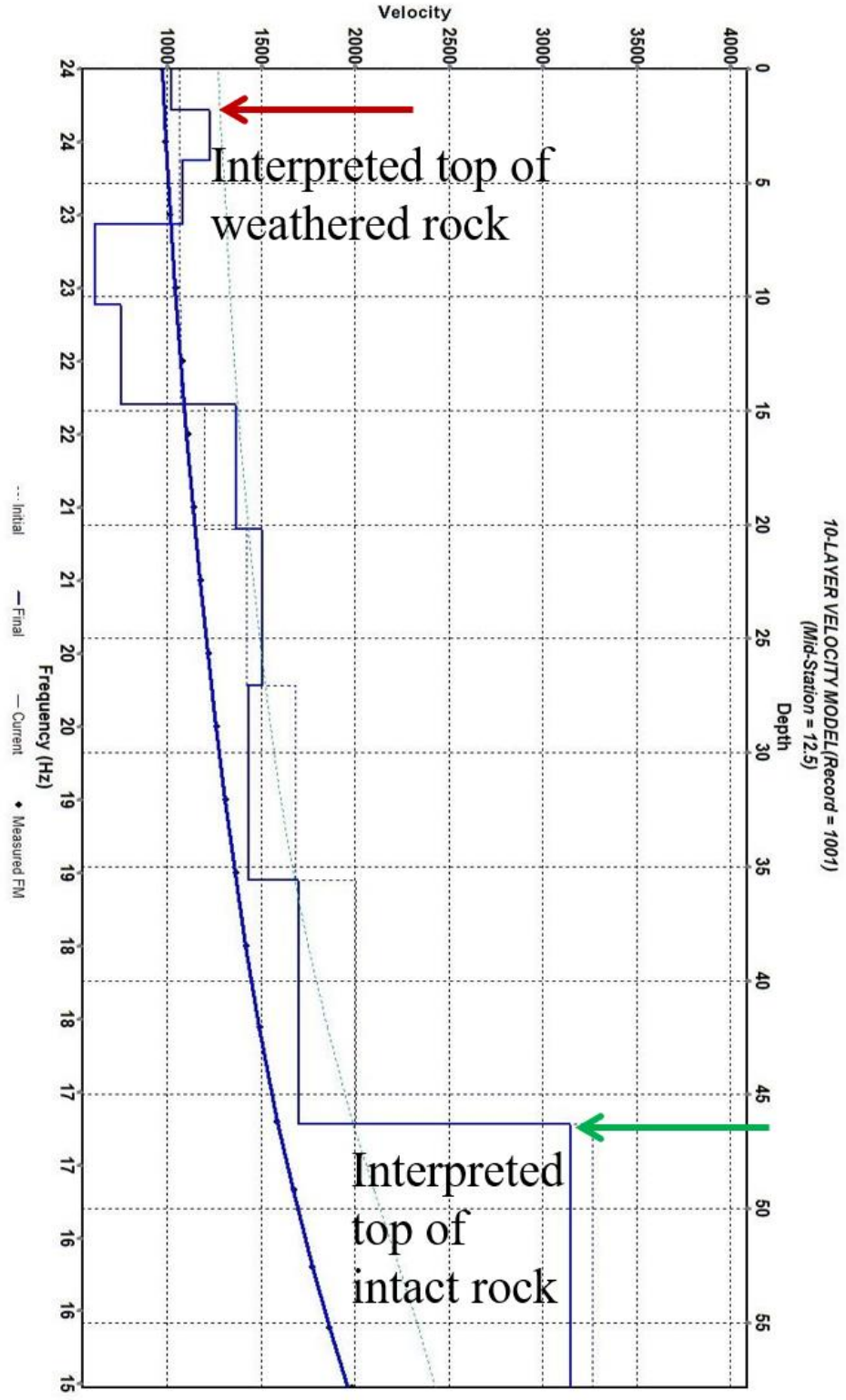
Velocity
1000
1500
2000
2500
3000
3500
4000
Interpreted top of weathered rock
Interpreted top of intact rock
10-LAYER VELOCITY MODEL(Record = 1001)
(Mid-Station = 12.5)
Depth
0
5
10
15
20
25
30
35
40
45
50
55
Frequency (Hz)
24
23
22
21
20
19
18
17
16
15
Initial
Final
Current
Measured FM

Profile 2

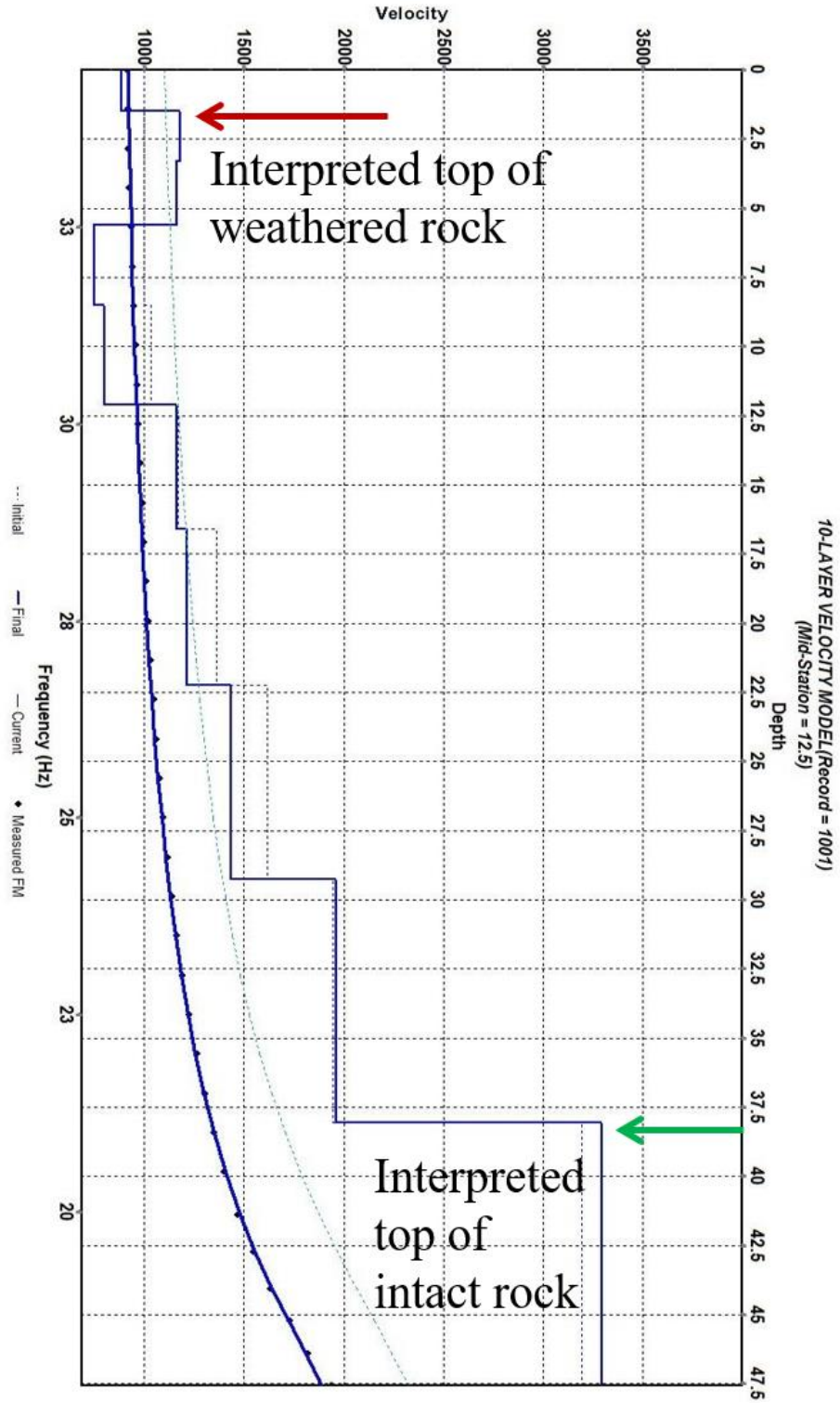
Velocity
1000
1500
2000
2500
3000
3500
Interpreted top of weathered rock
Interpreted top of intact rock
10-LAYER VELOCITY MODEL(Record = 1001)
(Mid-Station = 12.5)
Depth
0
2.5
5
7.5
10
12.5
15
17.5
20
22.5
25
27.5
30
32.5
35
37.5
40
42.5
45
47.5
Frequency (Hz)
33
30
28
25
23
20
Initial
Final
Current
Measured FM

Profile 3

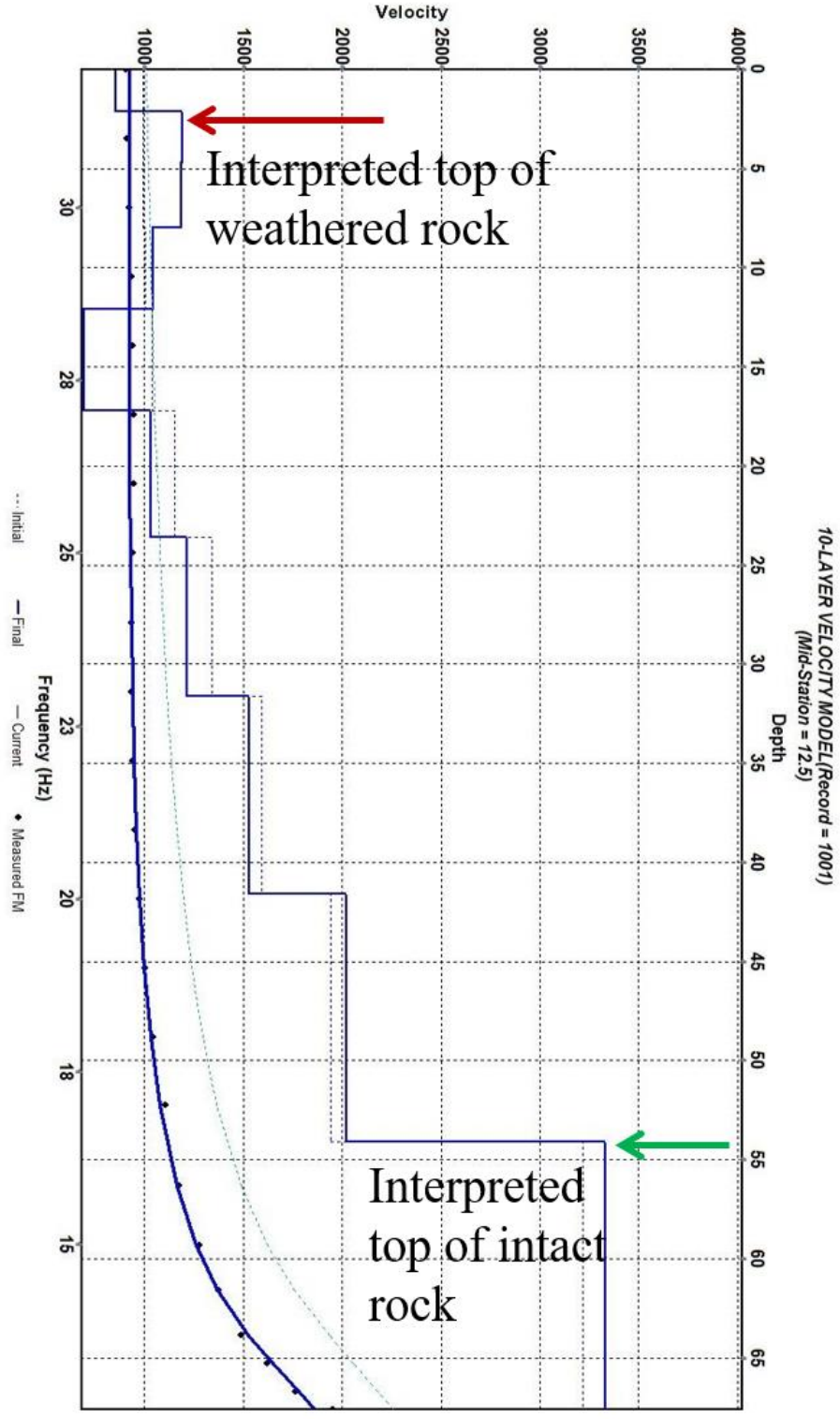
Velocity
1000
1500
2000
2500
3000
3500
4000
Interpreted top of weathered rock
Interpreted top of intact rock
10-LAYER VELOCITY MODEL(Record = 1001)
(Mid-Station = 12.5)
Depth
0
5
10
15
20
25
30
35
40
45
50
55
60
65
Frequency (Hz)
30
28
25
23
20
18
15
Initial
Final
Current
Measured FM

Profile 8

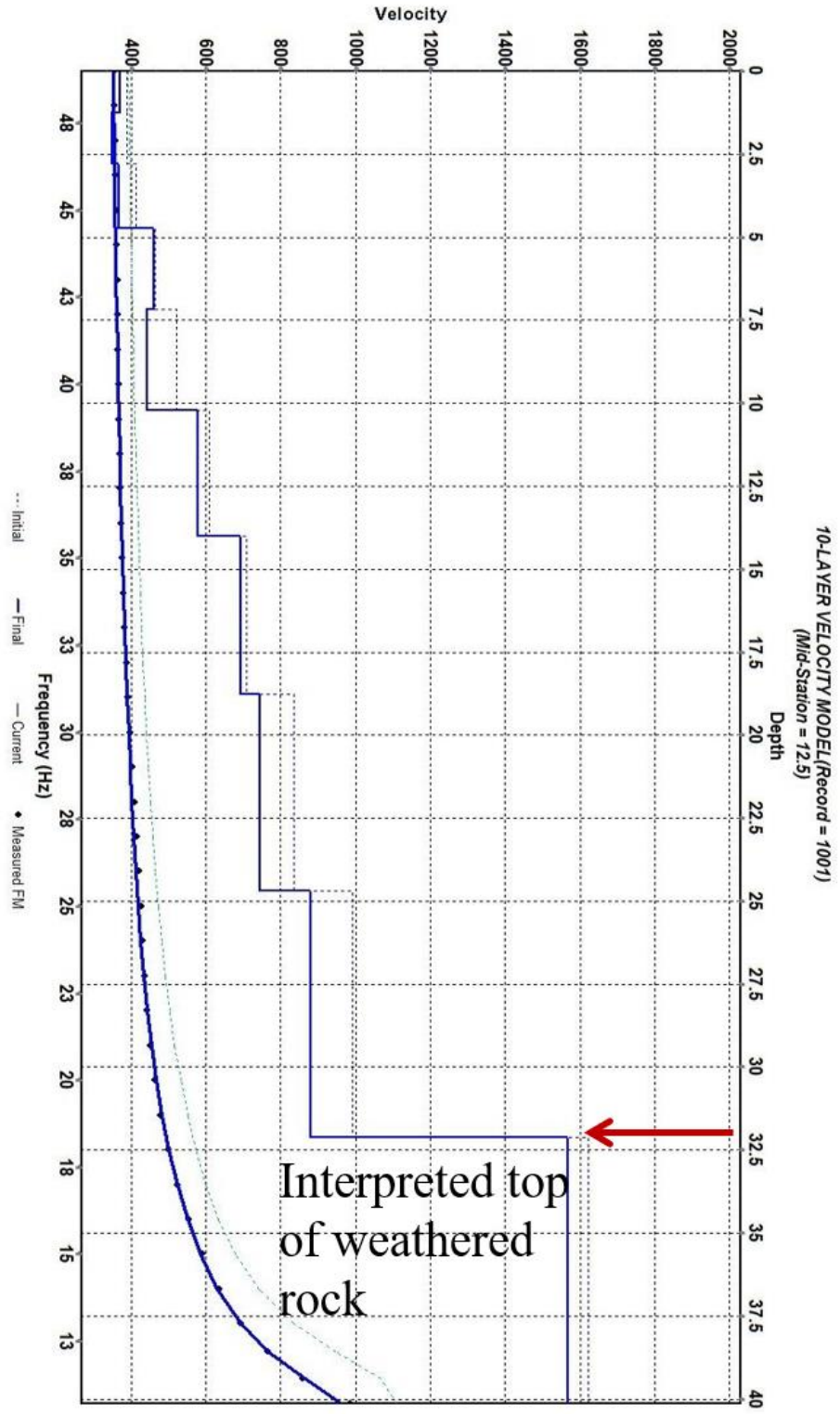
10-LAYER VELOCITY MODEL(Record = 1001)
(Mid-Station = 12.5)
Velocity
Depth
Frequency (Hz)
Initial
Final
Current
Measured FM
Interpreted top of weathered rock

Profile 9

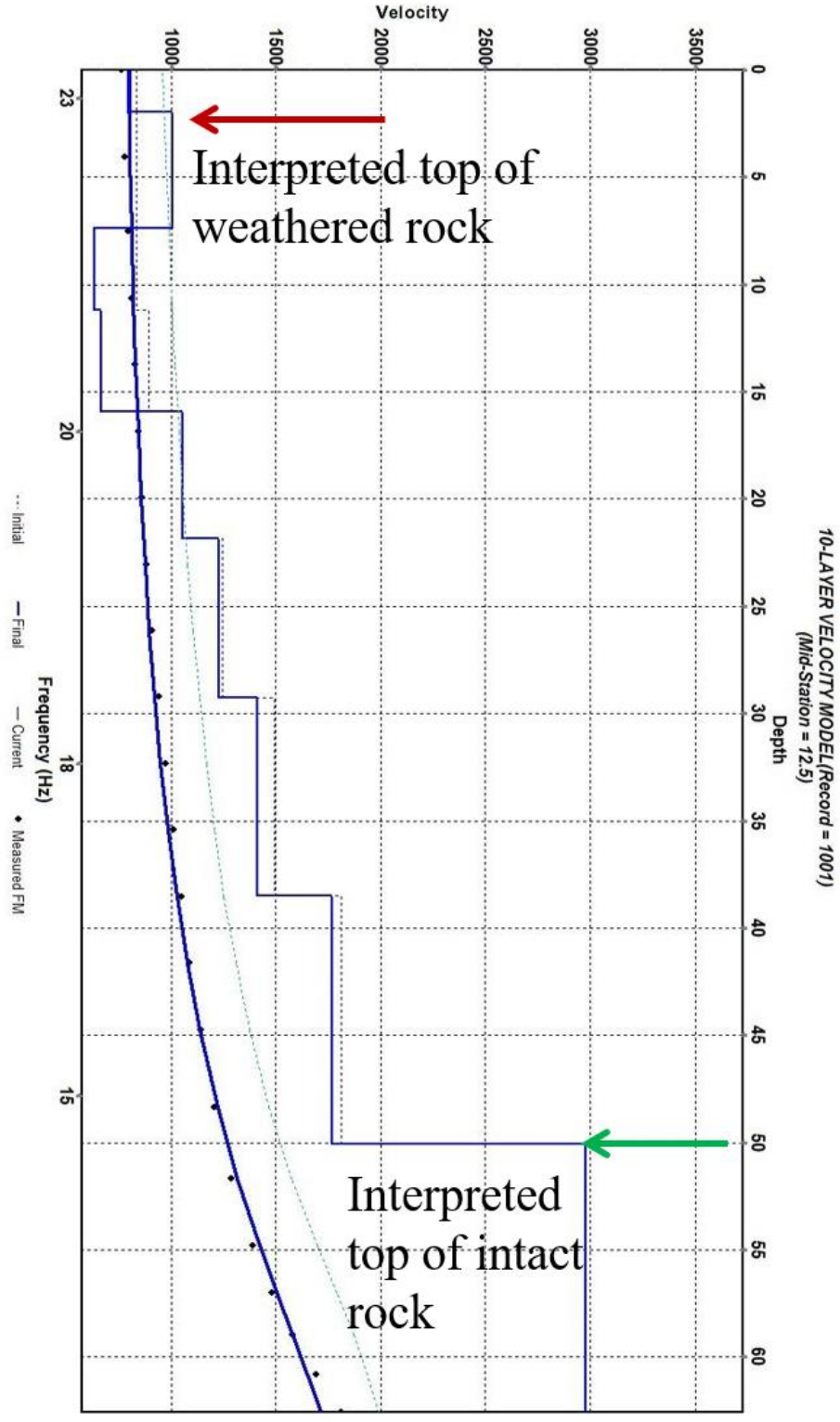
Velocity
1000
1500
2000
2500
3000
3500
Interpreted top of weathered rock
Interpreted top of intact rock
10-LAYER VELOCITY MODEL(Record = 1001)
(Mid-Station = 12.5)
Depth
0
5
10
15
20
25
30
35
40
45
50
55
60
Frequency (Hz)
23
20
18
15
Initial
Final
Current
Measured FM

Profile 11

BIBLIOGRAPHY

1. Anderson, N. L., Thitimakorn, T. (2004). A 2-D MASW shear-wave velocity profile along a test segment of Interstate I-70, St. Louis, Missouri. In 2006 Proceedings of the Highway Geophysics NDE Conference (pp. 594-608).

2. Anderson, N. L., Torgashov, E. (2018). Geophysical Investigation of Lake Chesterfield Site. Report prepared for; The Lake Chesterfield Home Owners Association. Prepared by; Bara Geophysical Services, LLC.

3. Corry, C. E., DeMoully, G. T. Gerety, M. T. (1982). Field procedure manual for self-potential surveys. Zonge Engineering & Research Organization, Tucson, Arisona.

4. Eckelkamp, R. M. (1986). Subsurface exploration – Dams and lakes, Lake Chesterfield St. Louis Country, Missouri. A report prepared for; Mason Group, St. Louis, Missouri. Prepared by; Geotechnology, Inc.

5. Erchul, R. A., Slifer, D. (1989). The Use of Self Potential to Detect Ground-Water Flow in Karst. Technical Report REMR-GT-6, U.S. Army Engineer Waterways Experiment Station, Vicksburg, MS.

6. Gercek, H. (2007). Poisson's ratio values for rocks. International Journal of Rock Mechanics and Mining Sciences, 44(1), 1-13.

7. Li, J., (2018). Imaging the subsurface in the eastern part of Lake Chesterfield using a combination of geophysical tools. A thesis, prepared for Missouri University of Science and Technology, Geological Engineering Department.

8. Loke, M.H. (2004) Tutorial: 2-D and 3-D Electrical Imaging Surveys. Geotomo Software, Res2dinv 3.5 Software.

9. Missouri Department of Natural Resources (2018). Sinkholes in Missouri. [Photograph] Retrieved from: https://dnr.mo.gov/geology/geosrv/envgeo/sinkholes.htm

10. Revil, A. Finizola, A., et, al. (2017). Geophysical investigations at Stromboli volcano, Italy. Implications for ground water flow and paroxysmal activity. Geophysical Journal International, Oxford University Press (OUP), 2004, 157, pp.426-440.

11. Robert, T., Dassargues, A., et, al. (2011). Assessing the contribution of electrical resistivity tomography (ERT) and self-potential (SP) methods for a water well drilling program in fractured/karstified limestones. Journal of Applied Geophysics 75(1): 42-53.

12. Taylor, D. G., (2005). Summary of work completed phase III. Exploration/grout curtain installation, Lake Chesterfield Dam. Report prepared for; Harbors at Lake Chesterfield Homeowners Association. Prepared by; Strata Services, Inc.

13. Wieners, M. A., Kremer, W. B., (2005). Exploration and repair summary report Lake Chesterfield dam and sinkhole Wildwood, Missouri. Report prepared for; Harbors at Lake Chesterfield Homeowners Association. Prepared by; Shannon & Wilson, Inc.

VITA

James Daniell Hayes was born in Auckland, New Zealand. In December 2006, he received his BSc degree in Science from the University of Waikato in Hamilton, New Zealand.

In August 2017, he received admission to study geological engineering (M.S) at Missouri University of Science and Technology in Rolla, Missouri, USA. He received his master of science in Geological Engineering from Missouri University of Science and Technology in December 2019.